Report Additional Thesis

Evaluation of the IH2VOF model for modelling of hydraulic properties near breakwater toes

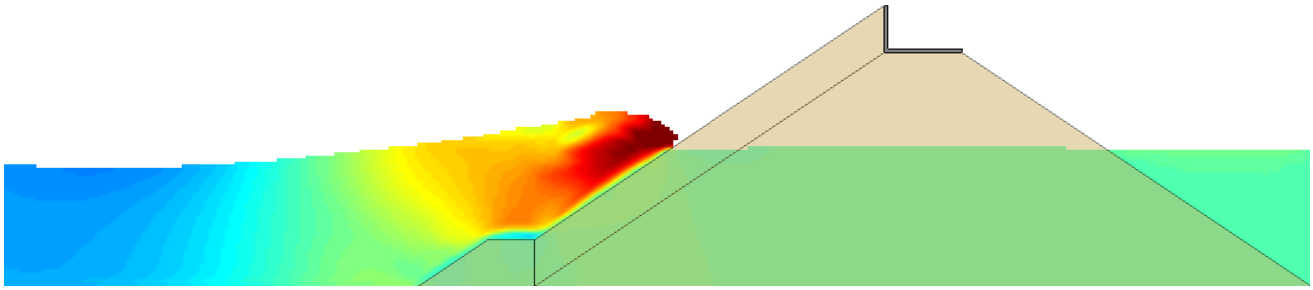

Author:
R.B.M. Peters
1357018

November 18, 2014

Preface

This report presents the results of my additional thesis which is part of my master Hydraulic Engineering at Delft University of Technology (DUT). The aim of this research is to determine the performance of the IH2VOF model when it is used to compute the local hydraulic parameters near the toe of a breakwater.

I would like to thank Ir. Henk Jan Verhagen (DUT) and Ir. Jeroen van den Bos (DUT and Royal Boskalis Westminster) who provided me with great input and views on my research. Furthermore thanks go to Senne Verpoorten, who was also investigating the IH2VOF model as part of his master thesis. It was very helpful to get acquainted with the IH2VOF model together, and without his help the simulations would have taken a lot more time.

Kind regards,

Ruben Peters
rbmpeters@gmail.com

Contents

1 Introduction **1**
1.1 Research goal . . . 1

2 Experimental set-up of the flume experiment **3**
2.1 Geometry . . . 3
2.2 Stone properties . . . 3
2.2.1 Basic stone properties . . . 3
2.2.2 Porous flow properties . . . 5
2.3 Hydraulic conditions . . . 6

3 IH2VOF model set-up **9**
3.1 Geometry breakwater . . . 9
3.2 Mesh requirements . . . 9
3.3 Convergence tests . . . 10
3.3.1 Flume length . . . 10
3.3.2 Grid cell width Δx . . . 12
3.3.3 Grid cell height Δy . . . 13
3.4 Interface between water and construction . . . 15
3.5 Hydraulic conditions for the IH2VOF model . . . 16

4 Comparison of the results **19**
4.1 Output parameters IH2VOF . . . 19
4.1.1 Horizontal flow velocity above the toe . . . 19
4.1.2 Free surface records . . . 20
4.1.3 Pressures . . . 20
4.2 Peak and trough comparison method . . . 21
4.2.1 Errors between the computations and measurements . . . 22

5 Conclusions and recommendations **25**
5.1 Conclusions . . . 25
5.2 Recommendations . . . 26

A Forchheimer experiment **27**

B Convergence test procedure **29**

C Peak and trough analysis **31**

D IH2VOF remarks **41**

Chapter 1

Introduction

A lot of research is performed on breakwaters and many of these researches use physical models to obtain the measurement data since this is a proven method. An alternative for physical models is the use of computer simulations to obtain the required data. Every year computers and computer models become faster and more accurate to the extent that some numerical models can be performed on normal computers. One of these numerical models is the IH2VOF model that was developed by Cantabria. This model can be used to simulate the water-land interaction and also incorporates the flow through porous media, and therefore seems like a real promising model.

1.1 Research goal

To determine to what extent the IH2VOF model can accurately simulate hydraulic conditions near toe structures of breakwaters

The IH2VOF model will be used to simulate wave flume experiments that were performed as part of the master thesis of the author. The results of the model will be compared to the measurements performed during the experiments. To achieve this the following steps will be taken:

- Determination of the geometry and parameters of the flume experiments required for the IH2VOF model
- Determination of the computational domain and required grid size
- Comparison of the model results with the measurements of the experiment for the following parameters

  Pressures just above the toe surface

  Pressures just under the toe surface

  Horizontal flow velocities above the toe

  Free surface elevation above the toe

  Free surface elevation in 'open water'

Chapter 2

Experimental set-up of the flume experiment

In order for the IH2VOF model to represent the experimental situation, certain input parameters are required. The geometry of the experimental set-up is an obvious requirement, but also the properties of the stones used in the breakwater are used in this model. The model uses these properties to calculate the flow through this porous interface. These properties have been determined by means of an experiment which is described in section 2.2.2. The goal of this experiment is to determine the porosity and the porous flow properties of the stones used in the breakwater.

2.1 Geometry

This thesis aims to validate the IH2VOF model by comparing the numerical results to actual measurements that were performed during the flume experiments performed as part of the master thesis of the author (Peters (2014)). Figure 2.1 shows the experimental set-up used during these experiments. EMS B and F are the velocity sensors at the toe and WG stands for wave gauge, which were located at the toe and 6 meters in front of the structure. Finally pA to pG indicate the pressure sensors.

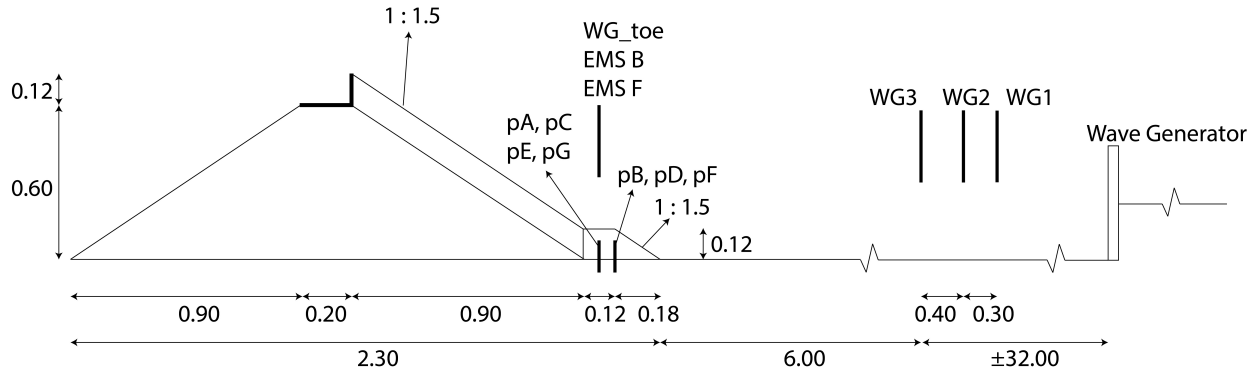

Figure 2.1: Experimental set-up of the flume experiment by Peters (2014)

2.2 Stone properties

The IH2VOF model needs several stone properties as input to perform its calculation. The more accurate these values are known, the better the comparability will be. Therefore these properties have been determined experimentally, rather than using approximate values that can be found in literature.

2.2.1 Basic stone properties

Nominal stone diameter

The nominal stone diameter $D_{n,50}$has been determined by weighing a sample of the stones (100-200 stones) and determining the sieve curves for the different stone classes. For each individual stone the diameter is determined with $D_n = \sqrt[3]{\frac{m}{\rho}}$. The sieve curve can then be created when the stones are ranked from lightest to heaviest and the cumulative weight percentage is plotted against the stone diameter. This results in the sieve curves that are presented in figure 2.2. From these curves the $D_{n,50}$can be determined by finding the diameter that corresponds with a cumulative weight percentage of 50%. The stone grading $\frac{D_{n,85}}{D_{n,15}}$ can also be determined by dividing the diameter corresponding to cumulative weight percentage 85% by the diameter corresponding with 15 %. The results are summarised in table 2.1.

Table 2.1: Nominal stone diameters and grading of the stones

Stone class	$D_{n,50}[m]$	$\frac{D_{n,85}}{D_{n,15}}$
Armour	0.044	1.39
Core	0.022	1.26
Toe	0.025	1.36

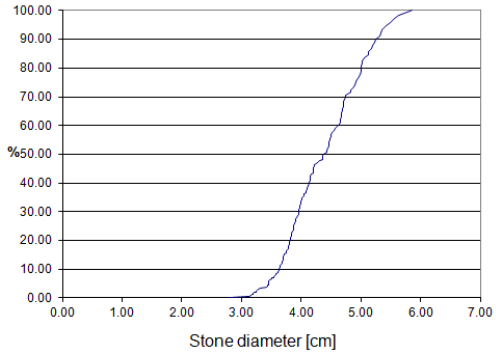

(a) Armour stones

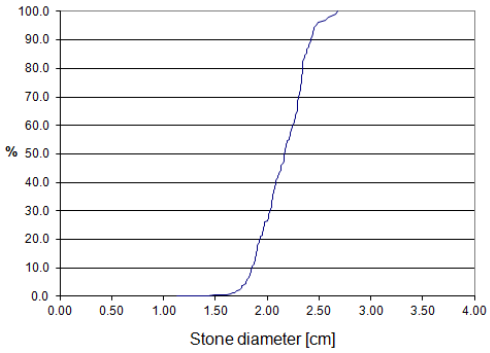

(b) Core stones

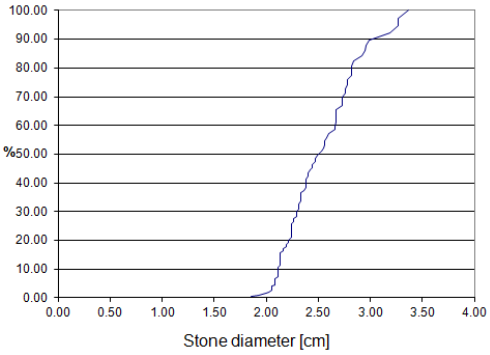

(c) Toe stones

Figure 2.2: Sieve curves for the three stone classes

Porosity

The porosity of stones can be determined by filling a bucket of known volume with stones and determine the weight. Thereafter water is added and the weight is determined again. The weight of the empty bucket and a bucket filled with water is also used to determine the total volume of the bucket. The porosity of the stones can then be determined by:

$$n = \frac{V_{water}}{V_{total}} \tag{2.1}$$

with $V_{water} = \frac{W_{mixture} - W_{stones}}{\rho_w}$ and $V_{total} = \frac{W_{water+bucket} - W_{bucket}}{\rho_w}$. The results are shown in table 2.2

Table 2.2: Determination of the porosity of the stones

Stone class	$W_{stones}[kg]$	$W_{mixture}[kg]$	$W_{water}[kg]$	$W_{bucket}[kg]$	$V_{bucket}[m^3]$	$V_{water}[m^3]$	porosity n [-]
Armour	28.08	37.48	19.37	1.10	0.0194	0.00940	0.49
Core	28.55	36.92	19.37	1.10	0.0194	0.00837	0.43
Toe	20.00	25.16	12.29	0.51	0.0123	0.00517	0.42

The porosity of the armour layer seems a bit higher than expected. An explanation for this is that a bigger bucket should have been used. The big stones cannot fill all the pores near the side of the bucket, so a larger porosity will be measured. However, during the flume experiments the armour layer was reinforced with a steel grating, which also resulted in larger pores than with simply dumped stones. It can therefore be argued that

the porosity of 0.49 does not reflect the properties of the stone class, but it does represent the armour layer used in the flume experiments. Even so, a test will be performed using a lower porosity for the armour layer, to check if significant deviations occur. The result of this test, shown in appendix C, is that the influence of changing the porosity of the armour layer was marginal with deviations of less than 1%.

2.2.2 Porous flow properties

Next to the basic stone properties the IH2VOF model also uses porous flow properties as input. These parameters are the linear friction coefficient α, quadratic friction coefficient β and added mass coefficient γ. The values for α and β describe the laminar and turbulent flow properties in between the stones respectively and have been determined experimentally during this research. The value for γ has not been determined experimentally so the standard value of $\gamma = 0.340$ that is given by IH2VOF will be used.

Theory

The flow through a porous medium can theoretically be determined by means of the Navier-Stokes equation, however this calculation would be enormous. Therefore simplified relations like the Forchheimer-equation (equation 2.2) have been established. These relations use average velocities over the porous media and friction coefficients. In general the various terms are combined in linear and quadratic friction terms (a and b respectively)

$$\frac{dh}{dx} = i = au_f + bu_f^2 + c\frac{\partial u}{\partial t} \tag{2.2}$$

$$a = \alpha\frac{(1-n)^2}{n^3}\frac{\nu}{g \cdot D_{n,50}^2} \tag{2.3}$$

$$b = \beta\frac{(1-n)}{n^3}\frac{1}{g \cdot D_{n,50}} \tag{2.4}$$

The Forchheimer equation uses the filter velocity u_f which is the porous flow velocity averaged over the total sample area (pores and grains). The third term in equation 2.2 is usually small and can therefore be neglected, which is the classical Forchheimer-equation (Schiereck (2004)). The coefficients a $[s/m]$ and b $[s^2/m^2]$ (and therefore the dimensionless coefficients α and β) can be determined experimentally, using the procedure explained in the following section. The value of α represents the laminar flow and β represents the turbulent flow regime. Both parameters are used as input parameters in the IH2VOF model and should therefore be determined.

From the Forchheimer equation the relation between the pressure gradient and the filter velocity is sometimes rewritten as:

$$u_f = k(i)^{\frac{1}{p}} \tag{2.5}$$

For the flow between small grains, like sand, ($D_{n,50} < 2 \cdot 10^{-3}[m]$) the flow has a laminar character and $p = 1$, reducing equation 2.5 to Darcy's law with permeability $k = a^{-1}$. For flow between larger grains or rocks ($D_{n,50} > 63 \cdot 10^{-3}[m]$), the flow is mainly turbulent and $p = 2$. For stone classes in between, like gravel, ($2 \cdot 10^{-3} < D_{n,50} < 63 \cdot 10^{-3}[m]$) the flow is in transition between laminar and turbulent. The stones used in the considered breakwater all fall in this category, but as turbulent flow is expected a value of $p = 2$ is chosen as input for equation 2.5.

Experimental set-up

The experiment was performed in the water cube in the Fluid Mechanics Laboratory of Delft University of Technology. It follows the experiment routine as performed by Koote and Zeelenberg (2012). The large cube serves as a water reservoir in which the experimental configuration is built. This configuration is a smaller reservoir on a pivot in which a sample of the stones can be placed. A controllable pump pump water from larger reservoir into the smaller one. The only way for the water to re-enter the larger reservoir is through the stone sample. The water levels in both the large and small reservoir are measured together with the discharge in the pipe connecting the two reservoirs.

The rationale behind this experiment is that the stone sample has a certain friction, therefore hindering the outflow of the water that is pumped into the small reservoir. Using this experiment these friction coefficients (a and b) can be determined. At the start of the experiment the water level in both reservoirs is the same (w.r.t. the bottom of the large reservoir) and the sample is submerged. During the experiment the pump starts pumping water from the larger to the smaller reservoir, causing the water level in the smaller reservoir to rise

and creating a water level difference between the two reservoirs. The bigger this height difference is, the bigger the discharge through the sample. For each pump setting there is an equilibrium in which the discharge through the sample is equal to the discharge through the pump and the water levels in both reservoirs remain constant. When this equilibrium is reached, the power to the pump can be increased which will lead to a new equilibrium position. This cycle is continued until the highest possible water level in the small reservoir is reached. During the entire experiment the discharge and the water levels in both reservoirs are measured.

Experiment results

The procedure in the section above was performed for the three stone classes: the stones used in the armour layer, the breakwater core and the toe. For each of these stone classes the porosity n, and the nominal stone diameter $D_{n,50}$ have been determined in the previous section, as these are input parameters in the Forchheimer equation. Using the material properties and the parameters measured during the experiments, the hydraulic gradient and the filter velocity can be determined. These values can be used to determine the permeability using equation 2.5 and the values for α and β. The results for the different stone classes are summarised in table 2.3. The complete analysis of the experiments can be found in Appendix A.

Table 2.3: Results of the permeability experiments

Stone class	$D_{n,50}[m]$	$n[-]$	$\alpha[-]$	$\beta[-]$
Armour	0.044	0.49	1826	1.70
Core	0.022	0.43	627	1.36
Toe	0.025	0.42	591	1.23

2.3 Hydraulic conditions

With the dimensions and properties of the experimental set-up known, only the hydraulic conditions that will be used in the numerical calculation have to be defined. During the core of the flume experiments of the author a total of 63 regular wave tests have been performed with the same experimental set-up, although a lot of these tests were re-runs of a certain set of hydraulic conditions. In table 2.4 all the different hydraulic conditions for this part of the thesis have been listed.

Table 2.4: Measurement campaign during Peters (2014)

Test	**h [m]**	**H [m]**	**s [-]**	**T [s]**
R001	0.30	0.12	0.04	1.39
R002	0.30	0.14	0.04	1.50
R003	0.30	0.12	0.02	1.96
R004	0.30	0.14	0.02	2.12
R005	0.30	0.16	0.04	1.60
R006	0.35	0.16	0.04	1.60
R007	0.35	0.16	0.02	2.26
R008	0.35	0.18	0.04	1.70
R009	0.30	0.14	0.04	1.50
R010	0.30	0.12	0.02	1.96
R011	0.30	0.12	0.02	1.96
R012	0.30	0.12	0.02	1.96
R013	0.30	0.14	0.02	2.12
R014	0.30	0.16	0.04	1.60
R015	0.30	0.14	0.02	2.12
R016	0.35	0.16	0.04	1.60
R017	0.35	0.16	0.02	2.26
R018	0.35	0.18	0.04	1.70
R019	0.35	0.18	0.04	1.70
R020	0.38	0.15	0.02	2.19
R021	0.38	0.17	0.02	2.33
R022	0.38	0.17	0.03	1.91
R023	0.38	0.19	0.03	2.01
R024	0.38	0.18	0.04	1.70

Continued on next page

Table 2.4 – continued from previous page

Test	h [m]	H [m]	s	T [s]
R025	0.38	0.20	0.04	1.79
R026	0.40	0.16	0.04	1.60
R027	0.40	0.18	0.04	1.70
R028	0.40	0.18	0.04	1.70
R029	0.40	0.20	0.04	1.79
R030	0.40	0.21	0.04	1.83
R031	0.40	0.18	0.03	1.96
R032	0.40	0.20	0.03	2.07
R033	0.45	0.20	0.04	1.79
R034	0.45	0.22	0.04	1.88
R035	0.45	0.20	0.02	2.53
R036	0.45	0.22	0.03	2.17
R037	0.45	0.22	0.03	2.17
R038	0.45	0.22	0.04	1.88
R039	0.35	0.18	0.04	1.70
R040	0.35	0.16	0.04	1.60
R041	0.35	0.16	0.02	2.26
R042	0.35	0.18	0.04	1.70
R043	0.30	0.14	0.04	1.50
R044	0.30	0.14	0.02	2.12
R045	0.30	0.16	0.04	1.60
R046	0.30	0.16	0.04	1.60
R047	0.38	0.17	0.02	2.33
R048	0.38	0.19	0.03	2.01
R049	0.38	0.18	0.04	1.70
R050	0.38	0.20	0.04	1.79
R051	0.40	0.18	0.04	1.70
R052	0.40	0.20	0.04	1.79
R053	0.40	0.21	0.04	1.83
R054	0.40	0.18	0.03	1.96
R055	0.40	0.20	0.03	2.07
R056	0.45	0.20	0.04	1.79
R057	0.45	0.22	0.04	1.88
R058	0.45	0.20	0.02	2.53
R059	0.45	0.22	0.03	2.17
R060	0.50	0.20	0.04	1.79
R061	0.50	0.20	0.02	2.53
R062	0.50	0.22	0.04	1.88
R063	0.50	0.24	0.04	1.96

Chapter 3

IH2VOF model set-up

3.1 Geometry breakwater

In order to be able to compute the hydraulic conditions near a breakwater toe in IH2VOF, the breakwater needs to be defined. This is done using CORAL, a GUI that is used to construct the breakwater, define the water levels and define the mesh. The program takes a little time to get used to and is somewhat counter-intuitive at some points, for instance the positive y-direction goes downwards. When defining a construction it is possible to create both solid media (*Obstacles*) and porous media. For the latter input is required regarding the stone size $D_{n,50}$, porosity n, added mass coefficient γ, and the values for α and β which are the laminar and turbulent porous flow properties respectively. All of these values have been determined in section 2.2, with the exception of added mass coefficient for which the default value of $\gamma = 0.340$ is used.

Figure 3.1 shows the breakwater that was constructed using CORAL, with a still water level of 0.30 m. If another water level is desired, or a longer flume length the mesh can be adapted by re-opening the file in CORAL. Another, faster, way is to open the mesh file in a program like notepad and change the coordinates in this file. In this file the mesh size and stone properties can also be altered, but special attention is required as there is no visual feedback using this method.

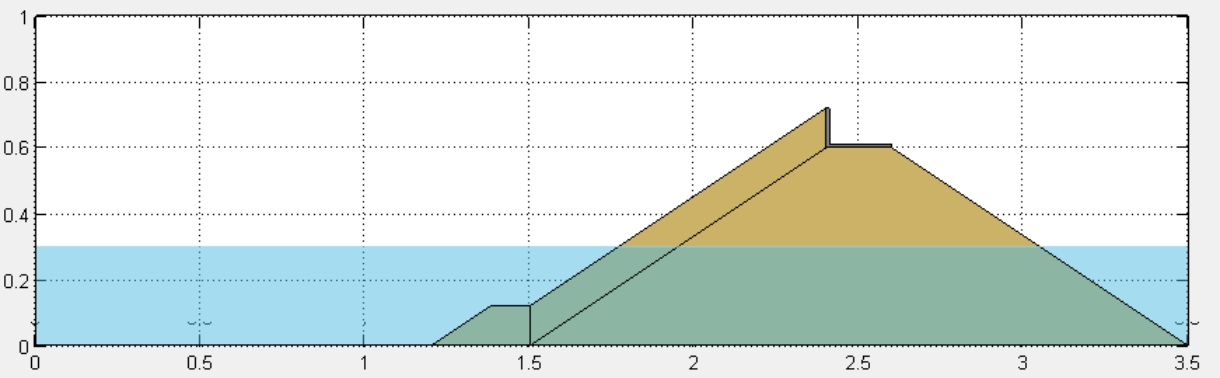

Figure 3.1: Breakwater model created in CORAL

3.2 Mesh requirements

The creators of the IH2VOF model have some guidelines for the mesh definition. The three parameters they mention are the computational domain, the mesh size in x (Δx) and the mesh size in y (Δy). For the flume length (L_f) it is recommended that it extends by at least half a wavelength from the structure:

$$L_{fe} > \frac{1}{2} \cdot L \tag{3.1}$$

For Δy it is advised that the wave should be vertically represented by at least 10 cells:

$$\frac{H}{\Delta y} \geq 10 \tag{3.2}$$

For Δx a relational requirement is given to prevent "false breaking" of the waves, which would happen if the steepness of the wave is too big. This yields to:

$$\Delta x < 2.5 \Delta y \tag{3.3}$$

In addition to this requirement the paper of van den Bos et al. (2014) recommend to use between 100-150 grid cells per wave length for reliable results. To be on the safe side this recommendation is defined as:

$$\frac{L}{\Delta x} \geq 150 \tag{3.4}$$

3.3 Convergence tests

The best way to compare the obtained test results with a numerical model would be to simulate the entire flume with a very detailed mesh, but this would lead to absurdly long computation duration. Therefore some optimizations must be found to reduce the computation time whilst still obtaining reliable results. To this goal several model set-ups are run to find the optimal set-up for the IH2VOF model.

In this thesis a lot of different hydraulic conditions will be simulated, and the chosen meshes should at the least comply with the recommendations given in the previous section. Therefore the limiting case should be found. From requirement 3.2 it follows that the lowest wave height leads to the finest required mesh. Requirement 3.4 shows that the shortest wave is the limiting condition for the grid cells in x-direction. The limiting case thus is the lowest and shortest wave. The corresponding test has a wave height of $H = 0.12$ m a water depth of $h = 0.3$ m and a period of $T = 1.39$ s. The wavelength was first estimated using the assumption of shallow water ($\frac{h}{L} < \frac{1}{20}$):

$$L = T\sqrt{gh} \tag{3.5}$$

This yields a wavelength of 2.38 m and this wavelength was used in the computations to determine the flume length. However since $\frac{h}{L} = \frac{0.3}{2.38} = 0.12 > \frac{1}{20}$ the shallow water equations should not have been used. Instead the equations for a transitional water depth ($\frac{1}{20} < \frac{h}{L} < \frac{1}{2}$) should be used for which the wave length can be determined by:

$$L = \frac{gT^2}{2\pi}\tanh(kh) \tag{3.6}$$

with $k = \frac{2\pi}{L}$ the wavelength is iteratively solved to be 2.13 m ($\frac{h}{L} = 0.14$).

Each of the tests will have the same hydraulic conditions (H=0.12 m, T=1.39 s, h=0.30 m) in order to be able to compare the results. The duration of each simulation is 100 s, which roughly corresponds with 50-60 waves that reach the structure. Each of these tests will have wave gauges on fixed positions which record the flow velocities and pressures at that x-position over the entire depth. After the tests from one of the three parameters (flume length, Δx, Δy) are finished, the flow velocities will be compared with each other. If the flow velocity of a test with a lower detail is not much different from the test with a higher detail the former test is deemed sufficiently reliable. A more detailed description of how these convergence tests are analysed can be found in Appendix B. All the tests in this chapter have been computer on a Windows 7 64-bit laptop with an Intel Core-i7-3612QM CPU @ 2.10 GHz, 4096 MB RAM and a solid-state drive (SSD). For the best performance it is advised to run a simulation on a single core with high priority (change the affinity and priority on the *Processes* tab in Windows Task Manager).

3.3.1 Flume length

In order to determine the optimal flume length several lengths are considered, based on the wave length. The first case is the recommendation which means that the flume extends half a wavelength in front of the structure. From here on the flume is lengthened in steps of $0.5L$ to the longest flume extension length $L_{fe}$of $4.5L$ in front of the structure. For these computations the shallow water wave length was used, which was incorrect, however the computations were already run and recomputing would take a long time. Therefore the analysis is performed using the shallow water wavelength. Since the difference between the two wavelengths is not that big, the analysis is still useful.

The nine tests with different flume length will use the same mesh sizes in order to be able to compare these tests. In y-direction Δy is determined by 3.2, using a wave height of 0.12 m $H/10 = 0.012$ m . Since the flume has a height of 1 m, Δy is chosen to be 0.0125 m since to get a total of 80 cells in y-direction rather than $83\frac{1}{3}$.

For Δx the recommendation of Jeroen van den Bos is used as the initial value to obtain $2.38/150 = 0.016$ m. Since it is desired to get a whole number of cells in x-direction $\Delta x = 0.014$ m is used. Another, unforeseen, benefit is that this value resembles the required grid cell width for the transitional water depth wavelength $2.13/150 = 0.014$ m.

All the different test set-ups are listed in table 3.1, in this table the total flume lengths is the width of the breakwater plus the flume extension.
Using the convergence test described in Appendix B, the most suitable flume extension length will be chosen. Figure 3.2 shows the maximum difference in peak velocity between the reference case ($L_{fe} = 4.5L$) and the

Table 3.1: Test set-ups for the convergence test of the flume length

L_{fe}/L	Total flume length [m]	$\Delta y[m]$	Number of y-cells	Δx [m]	Number of x-cells	Computation time [min]
0.5	3.50	0.0125	80	0.014	250	9:00
1	4.69	0.0125	80	0.014	335	14:30
1.5	5.88	0.0125	80	0.014	420	17:00
2	7.07	0.0125	80	0.014	505	21:30
2.5	8.26	0.0125	80	0.014	590	23:30
3	9.45	0.0125	80	0.014	675	25:30
3.5	10.64	0.0125	80	0.014	760	26:00
4	11.83	0.0125	80	0.014	845	30:30
4.5	13.02	0.0125	80	0.014	930	33:30

other cases. The large deviations just above the water level may result from the possibility that at the same point in time (using the shifted time) one case has a lower wave height than the other case. This means that one case computes a water velocity at that point, while in the other case there is no water present so the velocity is zero. The large deviations near the waterline are therefore not representative for the accurateness of a certain scenario. Still it is clearly visible that a longer flume corresponds better with the reference case than a short flume. This is no surprise, as in the longer flumes the waves flatten overtime and therefore the hydraulic conditions in a flume that is only slightly shorter than the reference case will be more similar. Keeping this in regard it still can be argued that the cases of 0.5-1.5 L perform worse than the longer wave flumes. Still further analysis is required to find the optimal flume length.

To this end the relative error is computed per wave gauge, by taking the maximum difference between the reference case and the current case at a certain peak and divide it by the value of the peak. This leads to the results that are depicted in figure 3.3. Figure 3.3a shows the relative error per wave gauge and it can be seen that the relative error is in the order of 10-20%. This figure, however, still gives no conclusive answer with the regard to the flume extension length to be used. From the cases of 3.0 L and longer, the relative error is less than 10 % which seems to be accurate enough.

Figure 3.3b finally shows the relative error plotted against the relative flume extension length L_{fe}/L. In this figure the relative error is shown for the gauges "at sea", the gauges at the toe and the average of all gauges. This information is used to analyze whether the relative error is constant over the flume and it can be seen that from $L_{fe}/L = 3.5$ on the relative error over the flume is rather constant. Therefore this flume extension length will be used in further analysis, resulting in a total flume length of about 10.65 m.

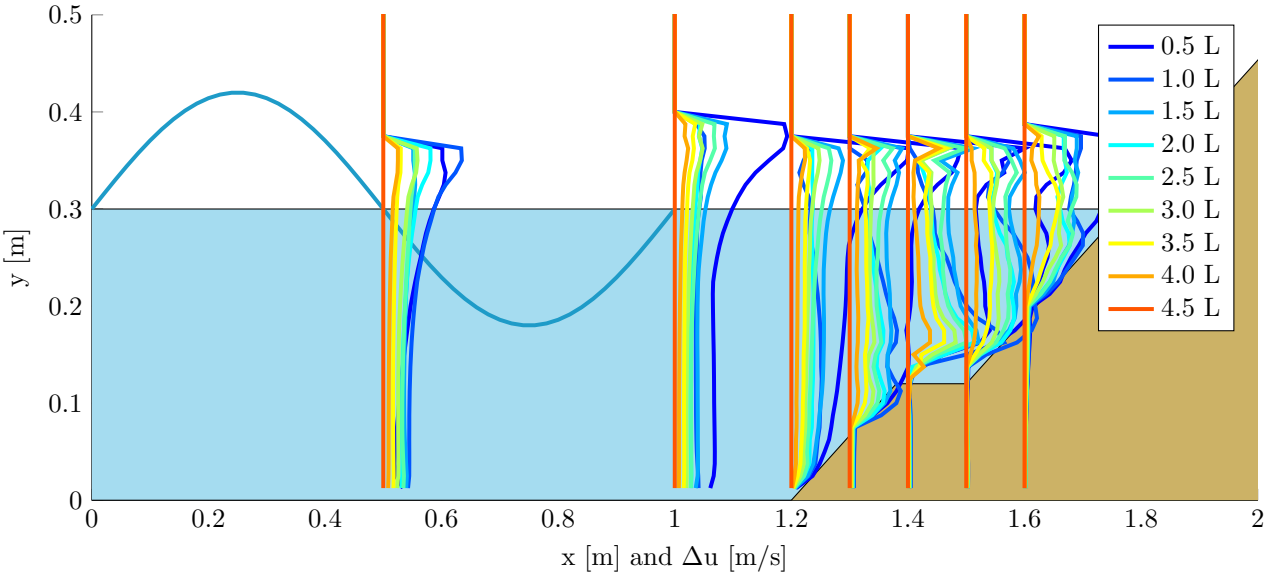

Figure 3.2: Differences in horizontal flow velocity with different flume lenghts

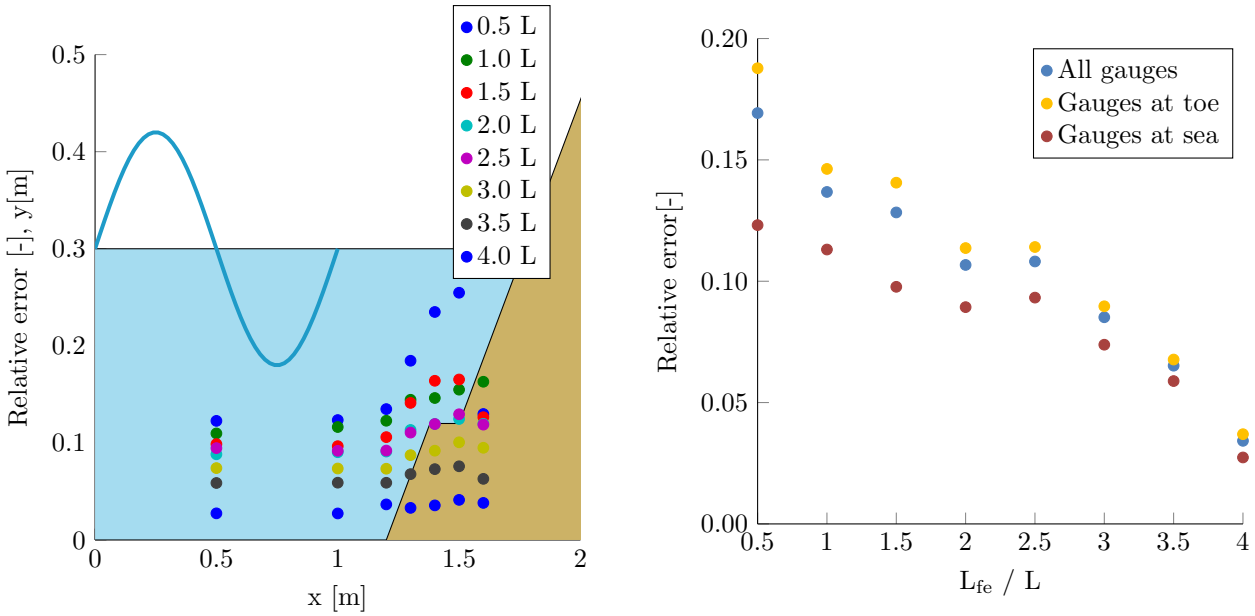

(a) Relative error over flume

(b) Relative error as function of L_{fe}/L

Figure 3.3: Relative error compared to the reference case of $L_{fe} = 4.5L$

3.3.2 Grid cell width Δx

With the flume length known, the next step is to determine the desired width of the grid cells in the mesh or Δx. A similar approach as the analysis for the flume length will be used. A flume of length 10.65 m with a constant y grid and wave conditions will be used where only Δx is changed. A total of five runs will be performed which are summarized in table 3.2.

Table 3.2: Test set-ups for the convergence test of Δx

$L/\Delta x$	Total flume length [m]	Δy [m]	Number of y-cells	Δx [m]	Number of x-cells	Computation time [min]
50	10.65	0.0125	80	0.0426	250	5:30
100	10.65	0.0125	80	0.0213	500	13:00
150	10.65	0.0125	80	0.0142	750	35:00
200	10.65	0.0125	80	0.01065	1000	63:00
250	10.65	0.0125	80	0.00852	1250	99:00

Figure 3.4 shows the maximal difference in computed horizontal flow velocities over the depth per wave gauge. It can be seen immediately that,except from the case $L/\Delta x = 50$, the differences are relatively small. This becomes clearer when looking at figure 3.5a and 3.5b, where relative error is depicted. The relative error at sea is not that different for the five cases, however the error differs quite a lot near the toe. Only $L/\Delta x = 200$ shows a more or less constant and small error over the entire domain and is therefore chosen as the best option.

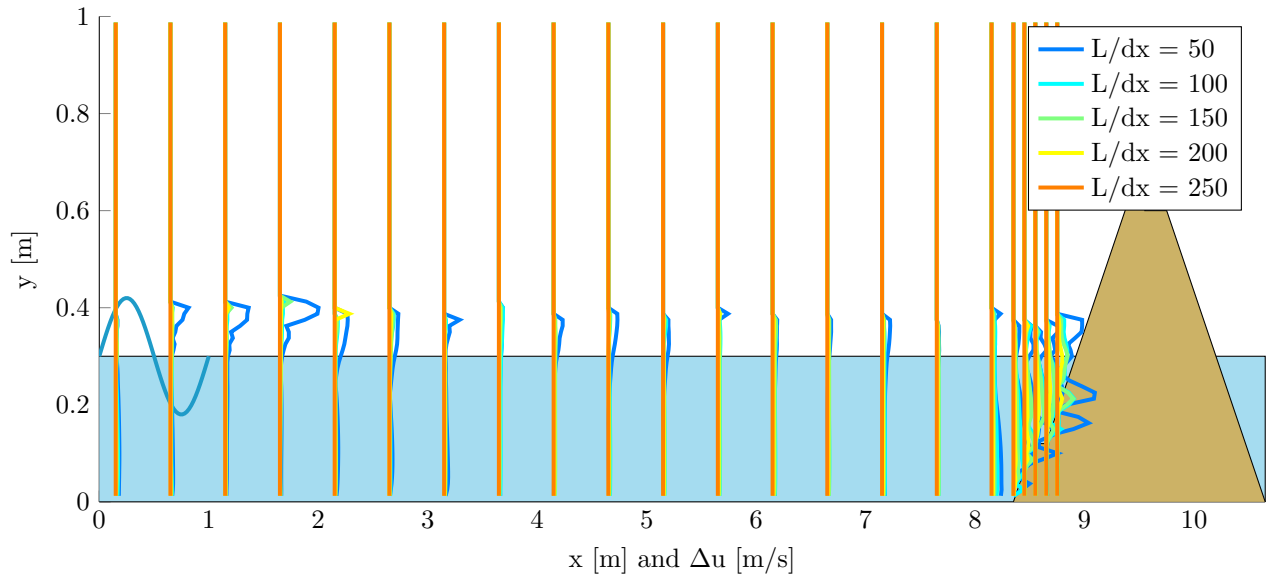

Figure 3.4: Differences in horizontal flow velocity with different Δx

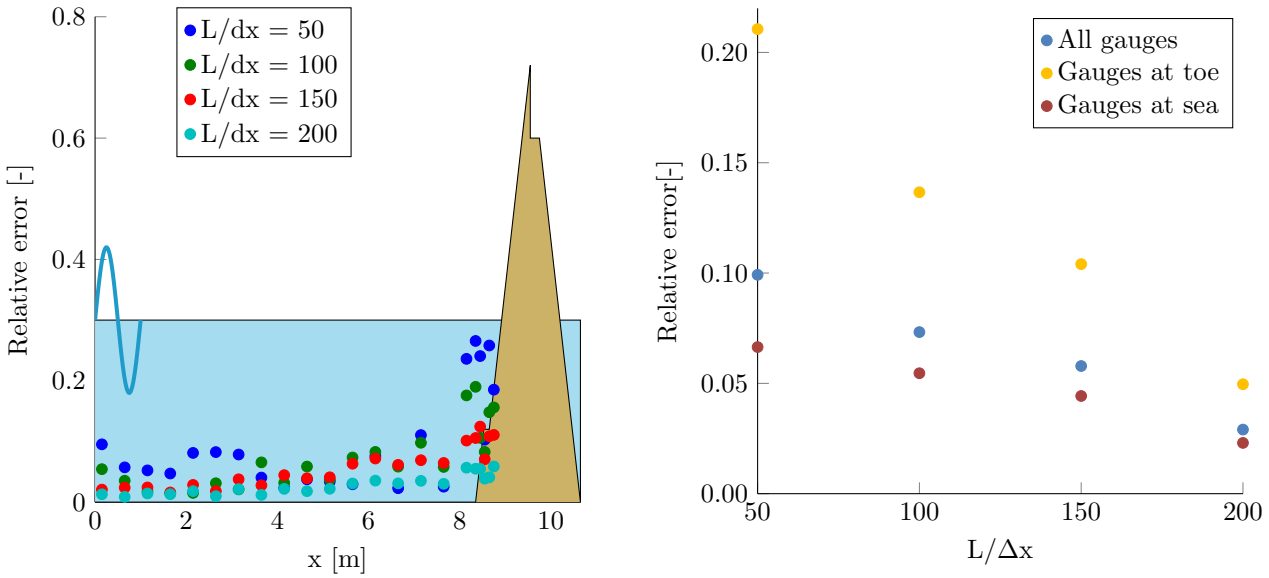

(a) Relative error over flume

(b) Relative error as function of $L/\Delta x$

Figure 3.5: Relative error compared to the reference case of $L/\Delta x = 250$

3.3.3 Grid cell height Δy

The last mesh parameter that needs to be determined in the height of the grid cell Δy. The four performed test set-ups are shown in table 3.3. For all of these runs the flume height was 1.008 m in order to end up with a whole number of cells in y-direction.
Figure 3.6 shows more differences than with the analysis of Δx, with $H/\Delta y = 5$ being the worst and the others which seem reasonably accurate. Figure 3.7a and 3.7b show that the relative error in all cases starts to grow near the toe, but $H/\Delta y = 15$ proves to be the most constant over the entire flume and is therefore chosen as chosen.

Table 3.3: Test set-ups for the convergence test of Δy

$H/\Delta y$	Total flume length [m]	Δy [m]	Number of y-cells	Δx [m]	Number of x-cells	Computation time [min]
5	10.65	0.024	42	0.01065	1000	19:00
10	10.65	0.012	84	0.01065	1000	59:30
15	10.65	0.008	126	0.01065	1000	113:30
20	10.65	0.006	168	0.01065	1000	179:30

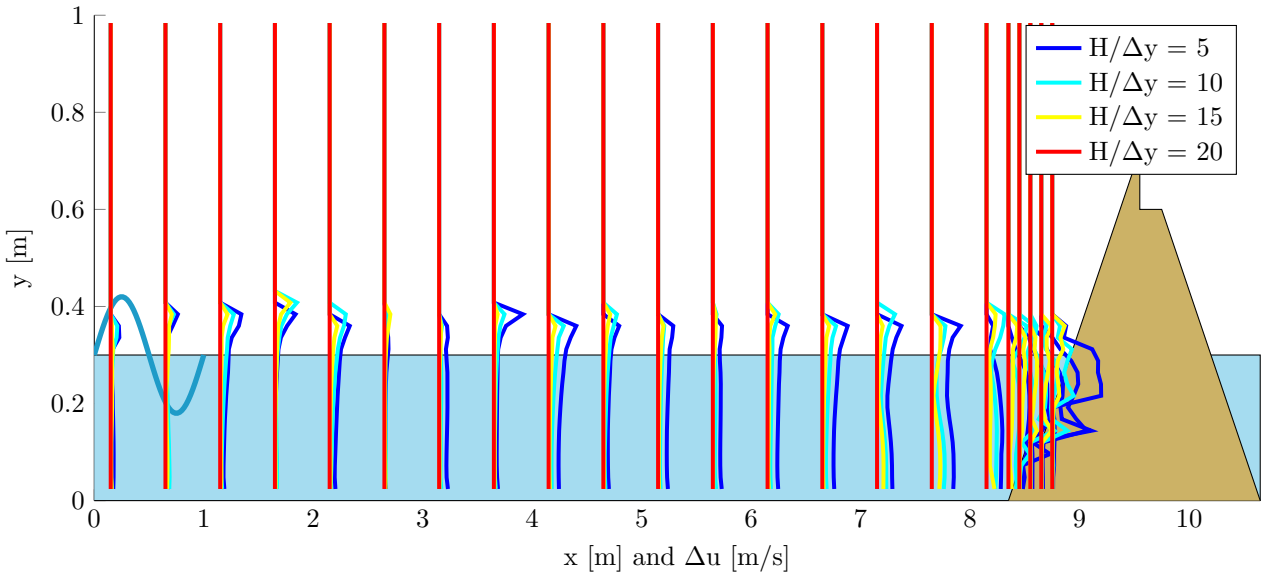

Figure 3.6: Differences in horizontal flow velocity with different Δy

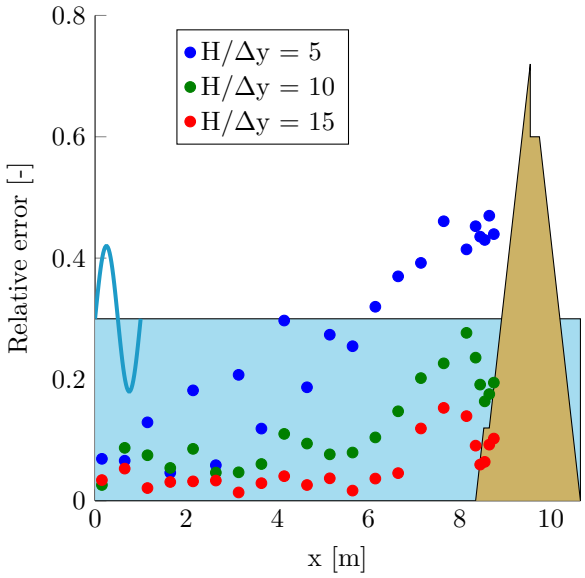

(a) Relative error over flume

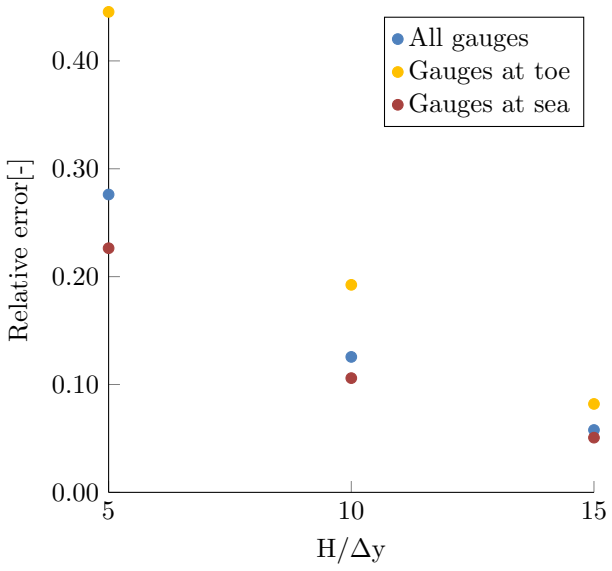

(b) Relative error as function of $H/\Delta y$

Figure 3.7: Relative error compared to the reference case of $H/\Delta y = 20$

3.4 Interface between water and construction

One of the focus points of this thesis is to determine if IH2VOF can determine the hydraulic conditions near the surface of a breakwater toe. Therefore it is of interest to zoom in on this area to check if the model can compute the hydraulic conditions in this area. To this end the *Drawfast* function of IH2VOF is used, which can be accessed in the *Postprocessing* menu of the IH2VOF GUI. This function allows the user to visualize the hydraulic conditions, by showing a movie-like animation of the velocities or pressures in every point for the duration of the test. To use this option the user has to indicate in the *Preprocessing* menu save the desired parameter for the entire domain. Drawfast is a very powerful tool which allows the user to quickly check the hydraulic conditions and get an idea of what is happening. The downside of this option is that a lot of data has to be generated (2GB per hydraulic parameter per 100 seconds using the mesh settings that were determined previously), whereas a 'normal' simulation with 15 wave gauges uses roughly 200-300 MB for a test period of 100 seconds. Moreover the computation takes much longer since the data-writing is a big time consumer in IH2VOF.

Using the meshsizes that were determined previously, a test run is performed wherein the hydraulic parameters are saved for the entire domain. Using the *Drawfast* option, the horizontal flow velocity near the toe is investigated. Figure 3.8a shows a detailed view of the toe and the velocities near it. The green colour near the toe indicates that the water velocity is nearly zero at that point, orange is roughly 0.4 m/s. This pattern can be seen throughout the test, the velocity up until roughly 1 cm above the toe construction always seems to be zero, and only above that layer the velocity shows the expected wave pattern. To determine the origin of this 'boundary layer', another test is performed which has the same properties and only differs in one aspect: instead of using porous stones a solid breakwater is created so the water cannot penetrate into the construction. A detailed view of the horizontal velocities near the toe for this case is shown in figure 3.8b and the problem can immediately be seen. Apparently the IH2VOF model cannot compute the hydraulic properties of a grid cell if that cell contains both water and piece of the construction. This makes sense as it would be hard to compute the flow trough a grid cell that consists of media with different flow properties. In this case the grid cells are roughly 1 by 1 cm, which corresponds with the size of the white spaces that can be seen in figure 3.8b. The obvious solution for this problem is to increase the resolution of the grid in order to compute the hydraulic properties just above the toe. The resolution should probably be about 4-5 times more detailed to be able to accurately compute the velocities just above the toe. As this would lead to an enormous increase in computation time, it is decided to continue with the grid cell dimensions as determined previously. During the analysis it should of course be taken into account that the computed hydraulic conditions within the band of 1 cm around the surface of construction are probably unreliable. Therefore the hydraulic parameters 'just above' the toe surface are evaluated at 2 cm above the surface, which is considered to be the reliable domain.

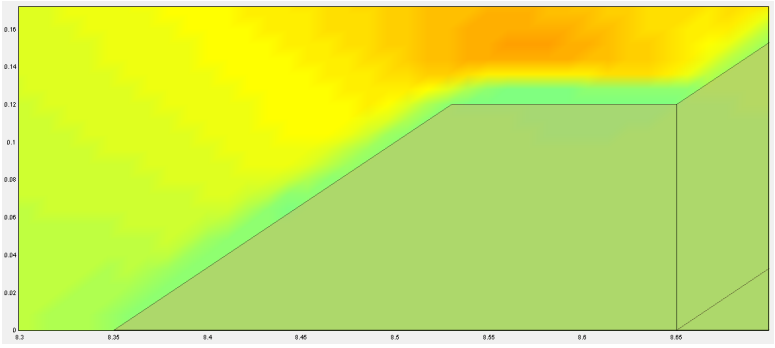

(a) Porous breakwater

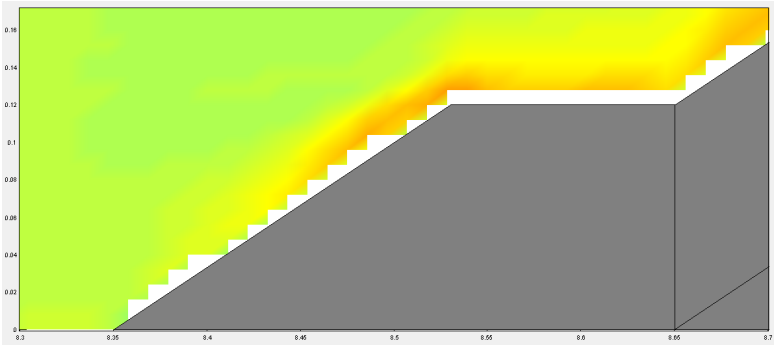

(b) Closed breakwater

Figure 3.8: Horizontal flow velocities above the toe. Green corresponds 0 m/s, orange with roughly 0.4 m/s

3.5 Hydraulic conditions for the IH2VOF model

The IH2VOF model allows for two ways to create a wave spectrum that will be used during a computation: generating a wave series by defining the wave characteristics (wave height, period, regular/irregular) or by reconstructing a wave series from a free surface record. Since a free surface record is available from the flume experiments, this seems to be the best option. By using this wave record the wave conditions should be more or less the same as the real case, whereas a generated (regular) wave series keeps repeating the same wave over and over again. To test if this is the case, case T005 has been computed in three ways. Option 1 uses a wave series that is generated by IH2VOF using the wave characteristics for this case (H=0.16, T=1.60). Option 2 uses the free surface record of R005 and option 3 uses the free surface record of R045. Although R005 and R045 have the same wave characteristics, the free surface records of these two experiments show some differences as can be seen in figure 3.9. This figure also shows the reconstructed wave series and because of the differences in free surface records, the reconstructed series also differ. The series for R005 has a lower wave height than R045, which is confirmed by IH2VOF which states that for R005 $H_s = 0.11m$ and for R045 $H_s = 0.15m$. Moreover it forces the wave into a harmonic form, so the height of the crests are more or less equal to the depth of the troughs. In the original signal the crests were notably higher than the troughs, so there is a discrepancy here.

Another possible difference between the reconstructed wave series and the original series is because of the reflection of waves. In the IH2VOF model waves will reflect on the breakwater and travel back towards the generator where they will be absorbed in the boundary. However the free surface record (on which the reconstructed wave series are based) is a measurement from the flume experiment so it already contains the reflective wave. Therefore it would seem that with the reconstructed wave series the reflecting will be accounted for twice, which does not represent reality. It is hard to prove whether this is the case, but it is something that should be kept in mind when opting for the reconstructed wave series rather than a wave series generated by IH2VOF.

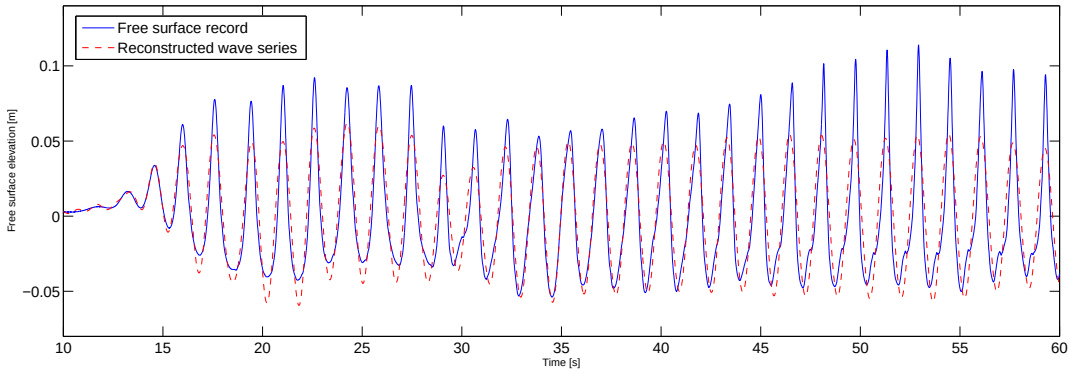

(a) R005

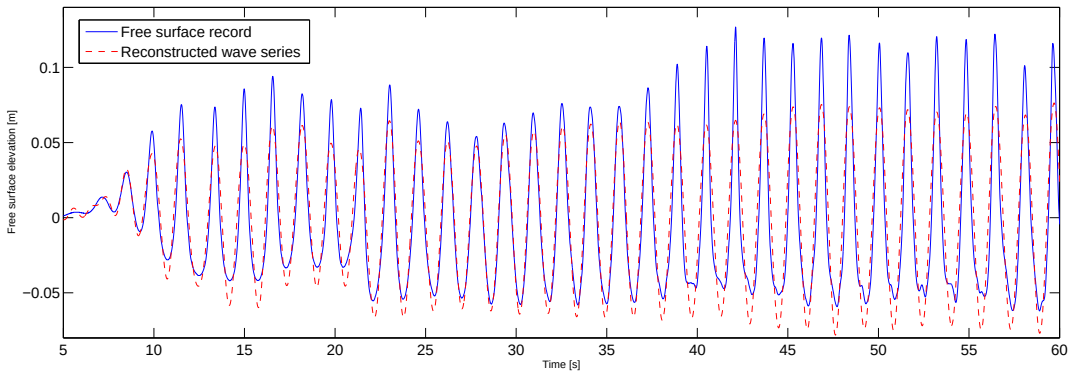

(b) R045

Figure 3.9: Reconstructed wave series

To check what method gives a free surface elevation which has the most resemblance to reality, the three options that have been mentioned earlier are analysed. The free surface records at the toe, obtained by IH2VOF are compared to the free surface record that was measured during the flume experiments. The results are displayed in figure 3.10. From this figure several observations can be made with respect to the different options.

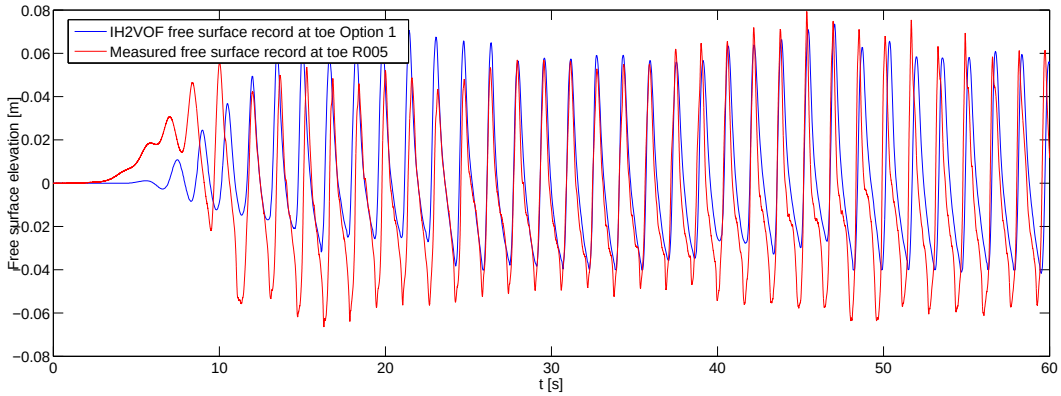

(a) Option 1a: Comparison of R005 with wave series generated by IH2VOF

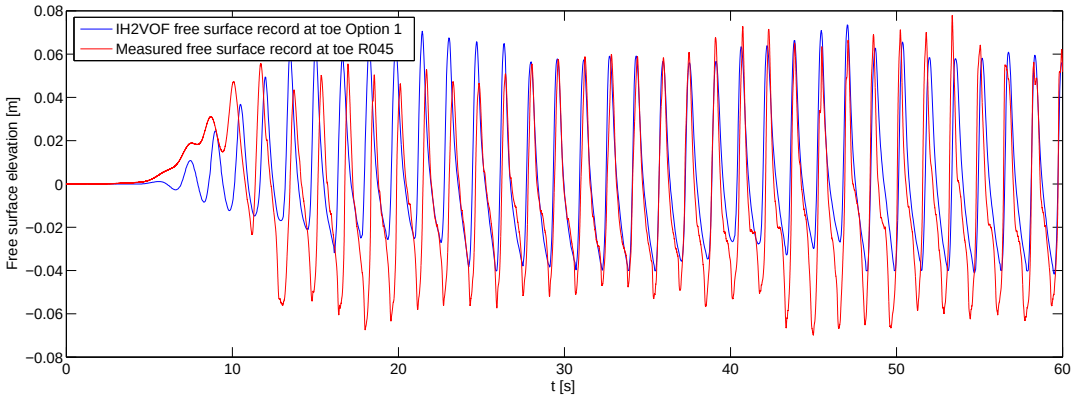

(b) Option 1b: Comparison of R045 with wave series generated by IH2VOF

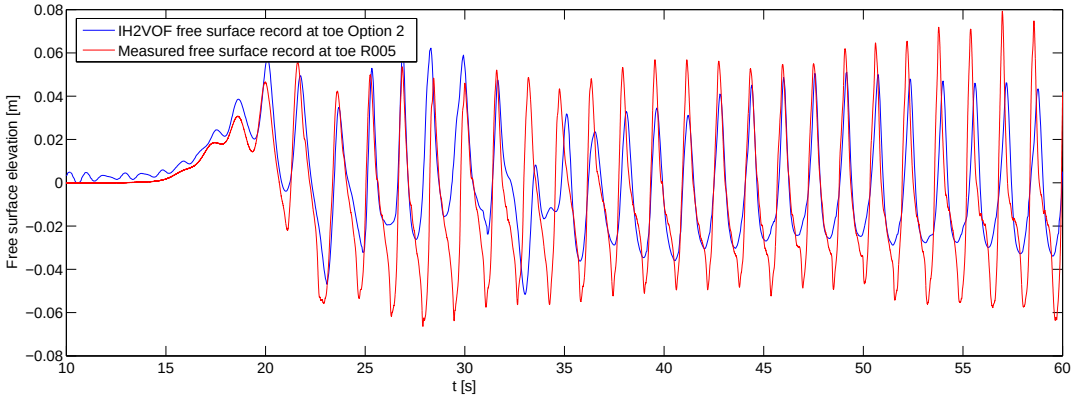

(c) Option 2: Comparison of R005 with wave series reconstructed from R005

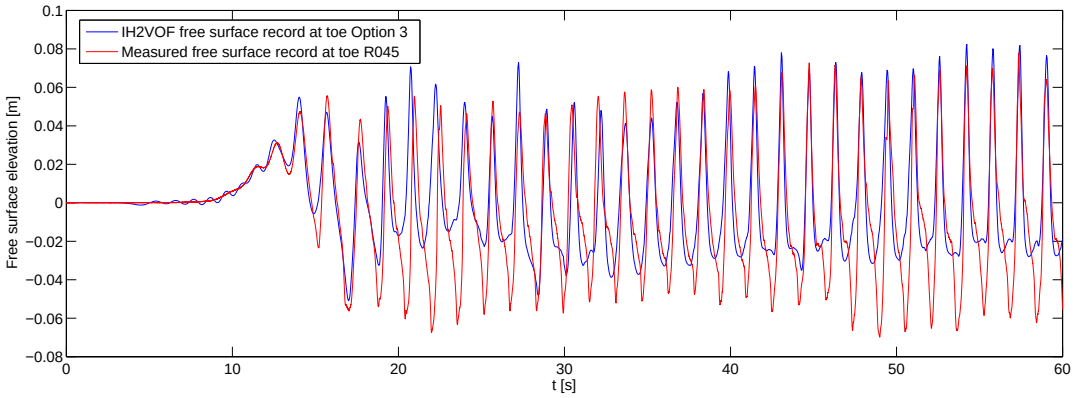

(d) Option 3: Comparison of R045 with wave series reconstructed from R045

Figure 3.10: Comparison of free surface records for the three options for wave series generation

Option 1 (wave series generated by IH2VOF) is compared to the measured values during R005 and R045 (figures 3.10a and 3.10b). It gives an overall good representation of the flume experiments. The peak values are an almost perfect representation of the real case after a spin-up period of approximately 30 seconds. The modelled troughs are generally too shallow with a typical deviation of 40-50%.

Option 2 (wave series reconstructed from R005) in figure 3.10c shows the worst results of the three options, with peaks that are too low and troughs that are too shallow. The typical deviations exceed 50% and should therefore be considered to be unreliable. An explanation for this observation is that the modelled waves are too low, which is the case since the reconstructed wave series had a significant wave height of $H_s = 0.11[m]$. This wave height is much lower than the wave height of $H = 0.16[m]$ which was asked from the wave generator during the flume experiments. It seems that reconstructing the wave series in IH2VOF does not replicate the wave series correctly in this case.

Option 3 (wave series reconstructed from R045) in figure 3.10d is an improvement when compared to Option 2. The peaks are almost modelled perfectly, as was the case in Option 1. The troughs are also too shallow in this case, with troughs that are twice (!) as shallow when compared to the measured values.

Although it would seem preferable to reconstruct a wave series from a measured free surface record, this analysis shows that there is a chance that this record is analysed incorrectly by IH2VOF resulting in a wave series that is very different from the real wave series. Therefore it is concluded that it is best to use the *create wave series* function of IH2VOF. The input parameters for the wave series are the same parameters that were used during the flume experiments. Since during those experiments some combinations of hydraulic conditions were tested multiple times, the amount of numerical runs will be less than the amount of flume experiments. During the flume experiments a total of 28 unique hydraulic combinations have been tested. Therefore 28 numerical calculations in IH2VOF will be performed, which are listed in table 3.4. Research of Arets (2013) has shown that if a certain simulation is repeated, the same results are obtained. This means that each simulation has to be performed only once. The simulations listed in table 3.4 were performed in a single night by using a separate computer for each simulation in a computer room at Delft University of Technology. This method was designed by Senne Verpoorten as part of his master thesis which ran simultaneously with this research.

Table 3.4: Unique hydraulic conditions used during Peters (2014)

Combination	$h[m]$	$H[m]$	$T[s]$	$s[-]$	$L[m]$	Represents experiments
T001	0.30	0.12	1.39	0.04	2.13	R001
T002	0.30	0.12	1.96	0.02	3.18	R003, R010, R011, R012
T003	0.30	0.14	1.50	0.02	2.34	R002,R009, R043
T004	0.30	0.14	2.12	0.04	3.47	R004, R013,R015,R044
T005	0.30	0.16	1.60	0.04	2.52	R005, R014, R045, R046
T006	0.35	0.16	1.60	0.02	2.69	R006, R016, R040
T007	0.35	0.16	2.26	0.04	3.99	R007, R017, R041
T008	0.35	0.18	1.70	0.04	2.89	R008, R018, R019, R039, R042
T009	0.38	0.15	2.19	0.02	4.00	R020
T010	0.38	0.17	1.91	0.02	3.43	R022
T011	0.38	0.17	2.33	0.02	4.29	R021, R047
T012	0.38	0.18	1.70	0.04	2.99	R024, R049
T013	0.38	0.19	2.01	0.02	3.63	R023, R048
T014	0.38	0.20	1.79	0.04	3.17	R025, R050
T015	0.40	0.16	1.60	0.02	2.84	R026
T016	0.40	0.18	1.70	0.04	3.05	R027, R028, R051
T017	0.40	0.18	1.96	0.04	3.61	R031, R054
T018	0.40	0.20	1.79	0.02	3.25	R029, R052
T019	0.40	0.20	2.07	0.02	3.84	R032, R055
T020	0.40	0.21	1.83	0.03	3.33	R030, R053
T021	0.45	0.20	1.79	0.03	3.41	R033, R056
T022	0.45	0.20	2.53	0.04	5.06	R035, R058
T023	0.45	0.22	1.88	0.04	3.61	R034, R038, R057
T024	0.45	0.22	2.17	0.04	4.27	R036, R037, R059
T025	0.50	0.20	1.79	0.04	3.55	R060
T026	0.50	0.20	2.53	0.04	5.31	R061
T027	0.50	0.22	1.88	0.04	3.77	R062
T028	0.50	0.24	1.96	0.04	3.96	R063

Chapter 4

Comparison of the results

4.1 Output parameters IH2VOF

For the runs listed in table 3.4 the IH2VOF model calculated the pressures, flow velocities and water heights at the locations of the gauges. The locations of these gauges corresponds with the location of the measurement equipment that was used during the flume experiments. The parameters that will be compared are the horizontal flow velocity 5 cm above the toe (u_{toe}), the free surface elevation above the middle of the toe (η_{toe}) and finally the free surface elevation near the beginning of the IH2VOF flume that corresponds to the wave gauge closest to the wave generator in the flume experiments (η_{wg}), the pressure at 2 cm under the stones at the front of the toe (p_{front}), the pressure at 2 cm under the stones in the middle of the toe (p_{middle}), the pressure 2 cm above the middle of the toe (p_{above}). Another important aspect that should be taken into account has to do with the fact that the IH2VOF is a two-dimensional model (xy), whereas the flume experiment is obviously three-dimensional (xyz). At a gauge location in the IH2VOF model, more than one 'real' gauge may be present. During the flume experiment two velocity sensors were used at the same x-y position above the toe. The same holds for the pressure sensors at the front of the toe (3 sensors) and in the middle of the toe (4 sensors). Therefore the average of the real gauges will be used in the comparison with the IH2VOF data.

In the following sections the output parameters of the IH2VOF model will be shown for test T005 and the corresponding measurements R005 and R045. This test was chosen as it very strongly shows the characteristic differences between the computations and the measurements as will be discussed in section 4.2. It may therefore seem that IH2VOF performs worse than is generally the case.

4.1.1 Horizontal flow velocity above the toe

Figure 4.1a shows a typical velocity record at 5 cm above the toe (which was the position of the velocity sensor in the flume experiment). As can be seen, there is a start-up period of about 45 seconds, after which the signal is stable. This period is the spin-up time of the model and will not be used in the comparison, as it is not representative for the results. The same holds for the pressure and free surface records and therefore it is chosen to use only use the data in the period from 45-100 s for the comparison. The data obtained by the flume measurements also shows some spin-up time, moreover data was recorded after the wave generator stopped. This means that the beginning and the end of the records should not be used in the comparison. In the end it was chosen to use the data that was recorded in between 100-155 s, therefore spanning the same period as the data that is used from the IH2VOF results.

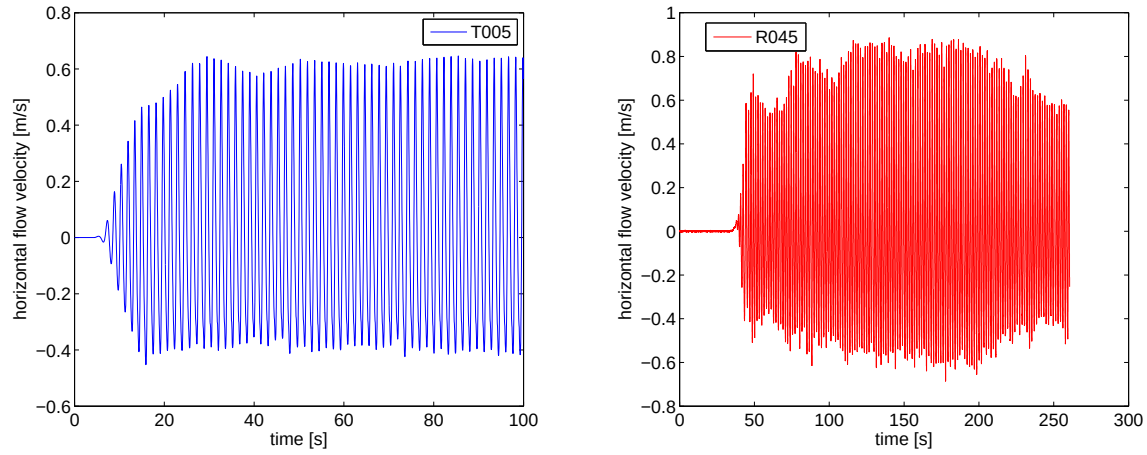

(a) IH2VOF *(b) Measurement R045*

Figure 4.1: Spin-up time for the IH2VOF model and the measurements for the horizontal flow velocity

Figure 4.2 shows the horizontal velocity record above the toe during the stable periods. The IH2VOF model shows a very stable wave pattern, which has lower peaks and troughs than the measured signal. The peak values are the velocities of the incoming wave and the trough values represent the return flow above the toe. Both of these velocities seem to computed too low by IH2VOF.

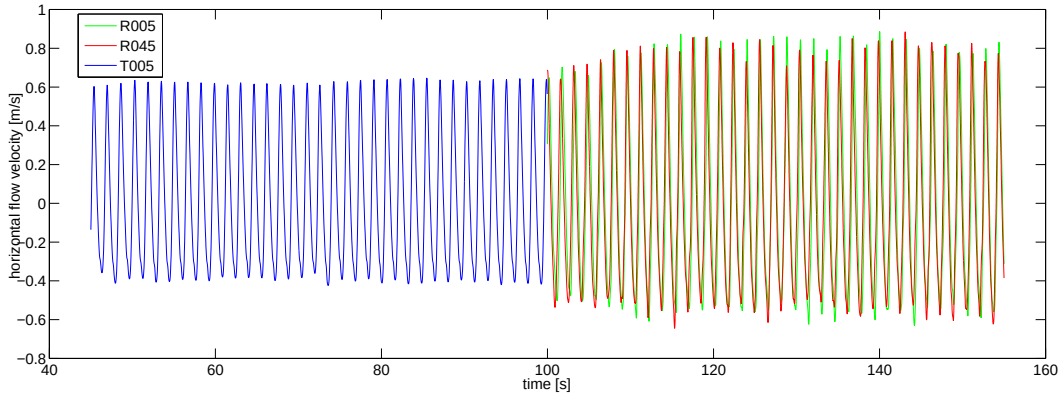

Figure 4.2: Horizontal flow velocity above the toe during the stable periods for T005, R005 and R045

4.1.2 Free surface records

Figure 4.3 shows the free surface record for test T005 and the corresponding measurements R005 and R045. It can clearly be seen that there is a vertical shift in the free surface record. The IH2VOF model shows more or less harmonic waves, whereas the waves that were actually measured are far more asymmetric. The total wave height (from trough to peak), however seems to be similar but this should be analysed later.

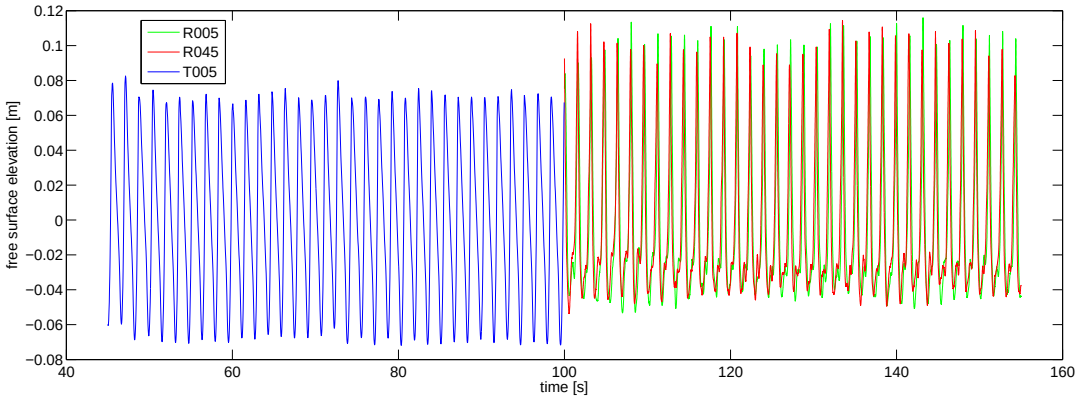

Figure 4.3: Free surface records closest to the wave generator for T005, R005 and R045

Figure 4.4 shows the free surface record above the toe. The peaks computed by IH2VOF are slightly lower than the peaks measured, but the biggest difference can be found in the troughs which much shallower than the measured troughs. This behaviour was observed earlier in section 3.5.

4.1.3 Pressures

Figure 4.5 shows the pressures under the stones at the front of the toe. IH2VOF consequently computes the pressures too high, and it seems that the total pressure difference between the peaks and the troughs is lower for the IH2VOF computations. The same behaviour is seen for the pressures under the stones in the middle of the toe. Finally figure 4.6 shows the computed pressures 2 cm above the toe, which are compared to the measured pressures. It should be noted that the pressure above the toe was not actually measured during the experiments, but was computed by using the measured flow velocity and free surface records. The differences between the computations and measurements are quite large, especially the difference in the peaks. It seems the pressure differences between the peaks and troughs are twice as big in the measurements.

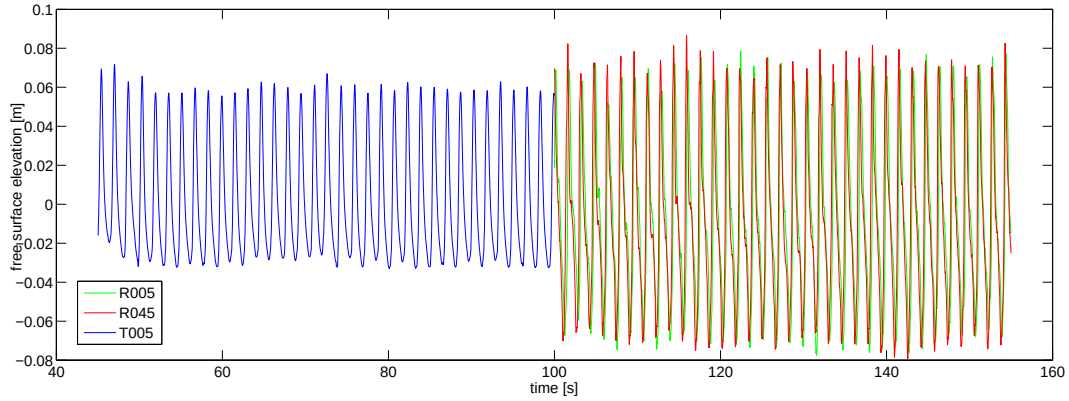

Figure 4.4: Free surface records at the toe for T005, R005 and R045

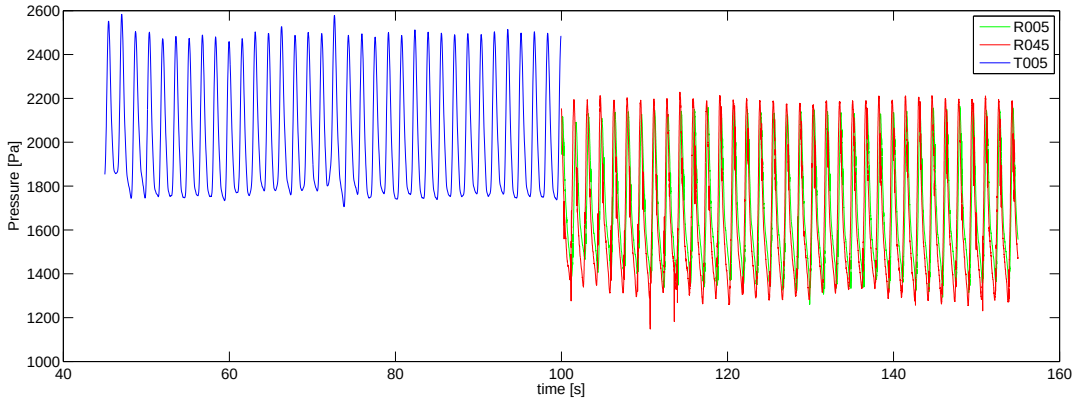

Figure 4.5: Pressures under the stones at the front of the toe for T005, R005 and R045

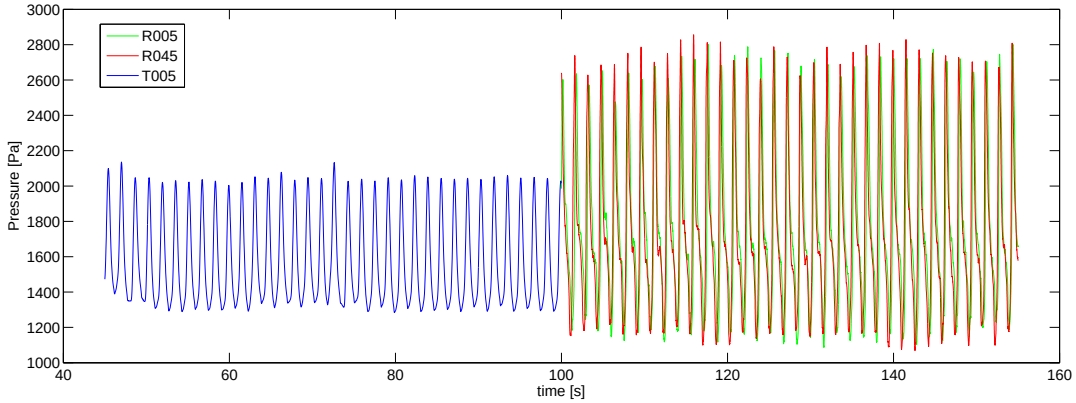

Figure 4.6: Pressures 2 cm above the toe for T005, R005 and R045

4.2 Peak and trough comparison method

Although a visual comparison can give a quick oversight of the differences between the measured and the computed hydraulic conditions, it is not a suitable method to compare large quantities of data. Therefore another comparison method is used which compares the peak (and trough) values for the different parameters. Using MATLAB, the peak values in the stable 55 second period of both signals are determined, yielding in a number of peaks N of roughly 25-35 (depending on the wave period) that can be compared. Thereafter the root-mean-squared (rms) is computed using equation 4.1. This equation shows the equation for the velocity, but a similar equation is used for the pressure and the free surface elevation.

$$u_{rms} = \sqrt{\frac{1}{N}\sum_{i=1}^{N} u_i^2} \tag{4.1}$$

The advantage of this method is that it yields in one characteristic value for each parameter of a computation or measurement, which makes comparison of the results very easy. The rms-values for all the measurements and computations presented in table C.2 and C.3. These tables compare the IH2VOF computations with the corresponding measurements. As was explained before some wave conditions have been tested multiple times, so one IH2VOF computation can be compared to several measurements. The differences between the computation and the measurements in percentage are also listed in tables C.2 and C.3, but will be discussed here.

4.2.1 Errors between the computations and measurements

With all the rms-values known, they can be compared to each other. Therefore the errors between the computations and the measurements have been computed by equation 4.2. A positive error thus means that the IH2VOF model computes a lower value for a parameter than was measured. Thereafter the average of the errors per IH2VOF run is taken, as there often is more than one measurement that corresponds with the computation. The resulting errors for the peak and trough comparison per IH2VOF run can be seen in table 4.1

$$error = \frac{u_{rms,measured} - u_{rms,IH2VOF}}{u_{rms,measured}} \cdot 100\% \tag{4.2}$$

It should be noted that the measurements R001-R014 are disregarded during the computation of the errors, since some small instruments errors occured during these experiments and therefore the results may be unreliable. For example in the computation of the average error for T004, only the errors for R015 and R044 are averaged. R001 and R002 only consisted of experiments in the range of R001-R014 and therefore they have been computed with these values, however the errors for T001 and T002 will not be used in further analysis of the errors because of the aforementioned concerns.

Table 4.1: Average errors in percentage per parameter per IH2VOF run

	Peak error [%]						Trough error [%]					
Test	u_{toe}	p_{front}	p_{middle}	p_{above}	η_{toe}	η_{wg}	u_{toe}	p_{front}	p_{middle}	p_{above}	η_{toe}	η_{wg}
T001	3.34	-19.47	-23.45	17.16	-0.47	27.97	17.72	-17.01	-14.67	1.99	38.34	-6.79
T002	16.78	-10.25	-9.96	25.87	26.60	34.32	3.94	-19.35	-26.62	5.51	16.74	-22.96
T003	11.51	-18.18	-18.70	18.82	-2.35	12.72	25.23	-25.46	-33.34	-11.36	61.70	-16.06
T004	19.92	-3.52	-2.05	33.57	51.18	9.38	-4.59	-14.04	-21.17	21.27	-4.72	-80.55
T005	22.43	-14.31	-13.62	25.16	19.20	30.62	28.06	-38.28	-45.24	-14.28	57.64	-57.98
T006	7.03	-13.55	-13.82	19.26	14.56	13.51	11.78	-15.99	-19.76	-7.93	47.76	-29.41
T007	30.01	-7.41	-6.25	25.07	10.77	18.87	-25.84	-16.07	-26.34	-0.99	28.82	-69.47
T008	18.15	-14.58	-13.77	20.60	23.38	37.90	21.17	-30.24	-33.87	-17.44	59.12	-5.03
T009	26.84	-4.31	-3.16	23.22	32.76	36.20	-12.44	-16.20	-24.52	1.75	24.99	-46.00
T010	1.17	-14.53	-14.60	16.10	-11.68	36.60	21.17	-16.26	-26.92	-3.53	37.44	-41.36
T011	21.78	-10.13	-6.93	19.10	-2.15	34.51	-20.47	-17.50	-27.81	-2.35	31.39	-72.45
T012	16.26	-10.97	-12.19	19.24	35.16	34.81	3.55	-15.43	-18.32	-7.76	35.77	-43.53
T013	16.18	-9.57	-9.25	24.16	34.70	36.45	10.83	-21.59	-29.59	-8.71	24.10	-48.12
T014	22.63	-11.49	-11.82	18.83	19.98	27.25	22.17	-27.93	-34.19	-18.25	55.80	-41.38
T015	1.66	-12.77	-15.12	7.45	-33.09	23.16	25.61	-14.22	-12.06	1.11	29.50	18.27
T016	14.77	-10.48	-11.41	18.63	38.01	36.11	8.59	-14.78	-17.73	-4.92	23.03	-41.26
T017	9.44	-11.34	-11.27	19.21	5.81	33.11	14.35	-19.35	-24.52	-5.58	24.26	-35.05
T018	21.02	-11.67	-12.29	18.04	20.69	32.86	26.77	-24.70	-28.62	-17.54	53.57	-34.35
T019	11.07	-9.24	-8.93	22.93	45.92	37.84	-10.83	-17.04	-22.78	-5.46	13.70	-85.67
T020	19.44	-12.18	-12.35	18.89	28.23	37.45	15.83	-26.17	-29.95	-19.15	52.87	-18.43
T021	16.47	-11.82	-13.01	8.10	-15.86	37.86	14.03	-12.38	-11.77	-6.55	36.32	1.03
T022	29.52	-7.08	-2.02	22.98	-0.64	-22.08	-6.66	-12.46	-14.64	5.64	40.04	-59.07
T023	15.69	-11.39	-12.15	13.55	6.38	39.60	21.56	-16.32	-21.97	-18.88	57.32	-30.24
T024	13.20	-8.63	-8.34	21.21	24.96	39.62	-13.26	-20.94	-31.06	-17.77	37.51	-44.26
T025	22.74	-10.71	-11.47	4.20	-32.58	37.79	-18.05	-10.78	-8.81	1.45	20.40	45.87
T026	38.80	-17.53	-6.12	19.60	-6.28	-19.20	-3.25	-9.64	-12.85	7.05	33.59	1.78
T027	13.30	-7.89	-8.40	13.07	15.58	0.57	7.67	-8.10	-6.56	1.00	23.88	-9.28
T028	31.62	-10.52	-11.89	14.33	21.72	25.01	-7.15	-15.84	-21.44	-13.47	48.21	-22.11

In order to get a more general insight in the performance of the IH2VOF model the mean of the errors in table 4.1 is taken (T001 and T002 excluded). This results in the expected error for a certain parameter. The mean error alone can give a distorted view of the performance of the IH2VOF model and therefore the standard deviation is also computed. For example: the error for η_{toe} for T008 is 23.38% (IH2VOF gives lower waves than

actually measured) and the error for T010 is -11.68% (IH2VOF gives higher waves than actually measured). The average of these two errors is $(-11.68 + 23.38)/2 = 5.85\%$, therefore showing a far more optimistic error than is actually the case. The standard deviation can be used to determine the spread of the error, and therefore checking if the value for the error is consistent. The relative standard deviation (RSD), which is the absolute value of the ratio between the standard deviation and the mean, can also be used for this purpose. Table 4.2 shows the mean errors, standard deviations and RSD-values for the peak and the trough comparison.

Table 4.2: Errors between the measurements and IH2VOF computations for the different parameters

Peak comparison	u_{toe}	p_{front}	p_{middle}	p_{above}	η_{toe}	η_{wg}
Mean error (bias) [%]	18.18	-10.99	-10.42	18.67	13.25	25.71
Standard deviation error [%]	8.87	3.42	4.11	6.12	21.91	17.24
RSD error [%]	49.82	31.19	39.41	32.77	165.41	67.05
Trough comparison	u_{toe}	p_{front}	p_{middle}	p_{above}	η_{toe}	η_{wg}
Mean error (bias) [%]	5.99	-18.37	-23.30	-6.26	36.69	-33.23
Standard deviation error [%]	16.44	6.92	9.04	9.73	16.29	30.51
RSD error [%]	274.26	37.68	38.79	155.58	44.40	91.81

It can be seen that for the peaks all parameters are modelled relatively consistent, with exception of the free surface record nearest to the wave generator and above the toe. The toe wave gauge is the worst, showing a standard deviation even larger than the mean error. This means that it is hard to predict whether the IH2VOF model computes waves that are too high or too low. The wave gauge nearest to the wave generator has a larger mean error, but its behaviour is easier to predict. In this case IH2VOF usually computes a lower wave height than was measured. The best computed values are the pressures under the stones, showing a relatively small error of about 10% with a standard deviation of about 4%. In all the cases IH2VOF computed slightly higher pressures than were measured, but the overall performance is very good. This means that the error can be accounted for by simply subtracting the error from the computed signal to get a better result for the pressures in the toe structure. The peak velocity above the toe (incoming flow) also performs reasonably well. Showing only positive errors, the computed velocity is always lower than velocities that are measured. The spread in the value for the error is a little too much to be able to conclude that the IH2VOF model can accurately compute flow velocities above the toe, but the results are not meaningless. Finally the pressures above the toe act reasonably well, despite the fact that they were measured at 2 cm above the toe, rather than just above the toe as was discussed in section 3.4.

In the trough analysis the pressure above the bed shows mixed results. Even though the mean error is quite small, the spread indicates that some uncertainty is to be expected. The same reasoning holds for the velocity troughs (return flow), which shows a very large RSD-value indicating a large spread in the error that can be expected. The pressures under the toe are, just as in the peak analysis, computed with the best consistency. Although the mean error is higher than the mean error of the peaks, the error is relatively consistent. Finally the wave troughs at both wave gauge locations show a large mean error and standard deviation. This was expected, since in section 3.5 it was observed that the wave troughs computed by IH2VOF were smaller (so the water level was higher)

Summarising the peak and trough analysis, it can be concluded that generally the computed velocities are too low, the pressures under the stones are too high, the pressures above the stones too high and the wave heights too low.

In section 4.1.2 it was observed that the computed wave height (distance from peak to trough) seemed to be very similar to the measured wave height. To verify this the sum of the rms-values for the peaks and troughs was taken for all computations and measurements yielding a characteristic wave height. The complete results are presented in table C.4, which shows that for most computations the error was indeed small (about 5-10%). The mean error (or bias) of all computations are presented in table 4.3. A positive error indicates that the computed waves are lower than the measured waves. The standard deviation, however, indicates that the error is not consistent, although the majority of the computations show a lower wave height. It seems the large RSD is caused by a few computations which show large errors (e.g. T022 -36.77%, T025 +41.51%), since most computations show errors of 5 to 10%.

Table 4.3: Errors wave height between IH2VOF and the measurements

	H
Mean error (bias) [%]	6.08
Standard deviation error [%]	15.82
RSD error [%]	260.27

Chapter 5

Conclusions and recommendations

5.1 Conclusions

The goal of this additional thesis was to determine if the IH2VOF model is capable of accurately computing the local hydraulic conditions near breakwater toes. During the research the IH2VOF model was configured and 28 computations were performed. These computations corresponded to a total of 63 actual flume experiments and an analysis was performed to find the differences between the IH2VOF model and the flume experiments.

Using the IH2VOF model is relatively user-friendly, the GUI that is used to configure the most important parameters for a test (wave series, position of wave gauges) works quite intuitively. The mesh and geometry of the breakwater are generated using CORAL, another GUI, which requires more time to get acquainted with. The convergence of model was tested for the three mesh parameters: the flume extension length, width of the grid cell Δx and the height of the grid cell Δy.

The analysis of the flume length showed no obvious convergence pattern, but it was decided to choose a flume extension length (distance from the beginning of the numerical flume to the construction) for which the relative error was more or less constant for all wave gauges. It was found that $L_{fe}/L = 3.5$, with L being the wave length of the limiting case, gave the best results and was therefore used in this research.

The convergence test for the required width of the grid cell Δx showed a very good convergence pattern with an increasing number of grid cells per wave length $L/\Delta x$, and it was concluded that a mesh width of $L/\Delta x = 200$ performed the best. The convergence test for the height of the grid cell Δy also showed a clear convergence pattern for larger numbers of grid cells per wave height $H/\Delta y$. It was found that $H/\Delta y = 15$ showed the best results.

An important aspect that should be kept in mind while using IH2VOF to determine the hydraulic properties near structures, is that there is some kind of boundary layer on the water-land interface. This thickness of this boundary layer is roughly the size of the grid cells. The reason for the presence of the boundary layer is that some of the grid cells on the surface of the construction contain both water and structure, which have different flow properties. IH2VOF is therefore not able to compute the hydraulic properties in this area, but it still gives a value for the different hydraulic condition (probably an average of the cells around). This means that the computed hydraulic conditions within the 'boundary layer' with the width of 1 grid cell, should not be trusted and thus not used in further analysis.

The performance of the IH2VOF model was evaluated by comparing the peak and trough values of the computations with those of the measurements for the the parameters under consideration. This was achieved by computing root-mean-square values for the peak and trough values, yielding a characteristic value for each parameter. By comparing these values several conclusions have been drawn concerning the different parameters:

Horizontal flow velocity above the toe
The IH2VOF model is generally quite capable of determining the horizontal flow velocity above the toe. The return flow seems to modelled the most accurate with an error of 6%, but the standard deviation of the error is quite large which means for some computations the error might be much bigger. The incoming flow has a higher error of 18%, but the spread in the errors is much less. The computed incoming flow velocity was always lower than the measured velocity. This means that it can be taken into account when analysing the IH2VOF results. Although the return flow generally shows computed velocities that are generally too low, in some computations they were too high so there is more uncertainty as to how to interpreted the IH2VOF results for the return flow.

Free surface records
During the analysis the free surface record was measured and computed at two locations, above the toe and near the beginning of the numerical wave flume. The wave gauge at the toe shows a mean peak error of 13%, indicating that the computed water level peaks at the toe are generally lower than the measured peaks. However there is a very large spread in this error, causing the computed value to be somewhat unreliable. The wave troughs are even more unreliable with a mean error of 37%, meaning that the computed troughs are less

deep than the troughs that are measured. Combining the information of the peaks and the troughs it can be concluded that the computed wave height at the toe is almost certainly too low, mainly because the troughs are not deep enough. It is however is hard to estimate what the error for an individual computation is.

The second free surface record was computed near the beginning of the numerical wave flume at 6.7 meters from the breakwater and was compared to a real wave gauge which was also positioned 6.7 meters in front of the breakwater. This position gives a very different result than the water levels at the toe. The peaks of the waves are still computed too low with a mean error of 26%, but the troughs are too deep with a mean error of 33%. This means, however, that the computed wave height (distance between the troughs and the peaks) is only a little lower than the measured wave height with a mean error of 6%. It must be noted that there is some spread in this error, sometimes indicating that waves are computed too big, but generally the waves are only slightly lower than the measured waves.

Pressures
The pressures were evaluated at three locations: 2 cm under the toe surface at the front of the toe, 2 cm under the toe surface at the middle of the toe and 2 cm above the middle of the toe surface. The first two locations under the toe show very similar results, which is logical as they were only space 6 cm apart from each other. The pressures in the toe construction are computed with an overall reasonably good accuracy with a peak error of 11% and 10% and a trough error of 18% and 23 % for the front and the middle respectively. Both the peaks and the troughs are computed too high. The peak and trough errors may seem like a lot, but because the spread in the errors is very low (especially for the peaks), the error is very consistent. This means that the error can be accounted for by simply subtracting the error from the computed signal to get a better result for the pressures.

As was pointed out before the IH2VOF model is unreliable in the boundary layer on the construction with a thickness equal to the grid cell dimensions. For the pressures just above the toe it was therefore chosen to compute these at 2 cm above the bed, whereas the measurements evaluates the pressure just above the bed at 3.5 mm above the bed. Still the pressures were evaluated, yielding in a surprisingly reasonable result. The pressure peaks are computed too low with an error of 19%, but the spread in errors is quite little, meaning the error can be accounted for. The pressure troughs generally are a little higher than the measured troughs usually and have a reasonably mean error of 6%

Summarising these results it can be concluded that IH2VOF performs reasonably well at computing the hydraulic properties near breakwater toes. Since a lot of the computed errors are relatively consistent they can be accounted for in further analysis.

5.2 Recommendations

Since a great part of this research consisted of working with the IH2VOF model, several recommendations for its future use can be made. Furthermore some general remarks and tips for the IH2VOF model are given in appendix D.

One of the most determining factors for numerical models is the computation time. In the ideal case a very detailed grid size would be used, but since this would lead to very long computation times this is not realistic. Therefore it would be advisable to try and make the model operate more efficiently. This research was performed simultaneously with the master thesis of Senne Verpoorten, and he has made some improvements to the program and made it possible to remotely compute a batch of simulations on different computers. It is therefore strongly advised to anyone who will use the IH2VOF model in the future to look into his work which will be published in 2015.

Another recommendation is to look into new ways of creating a fitting wave series input for the wave generator of IH2VOF. As was discussed in the conclusion the computed wave heights and velocities were usually too low, maybe with a different wave input they would correspond better with the flume experiments. For example if the user wants to simulate a wave height of 0.16 m, maybe it should be defined as 0.17 m to get to a resulting computed velocity or wave height that corresponds better to the reality. The main problem seems to be that the IH2VOF model forces the waves to be harmonic, whereas the waves in the flume experiment were asymmetric with lower troughs and higher peaks.

Appendix A

Forchheimer experiment

This appendix describes the analysis of the Forchheimer experiment that was performed, based on the simplified Forchheimer equation:

$$\frac{dh}{dx} = i = au_f + bu_f^2 \tag{A.1}$$

with

$$a = \alpha \frac{(1-n)^2}{n^3} \frac{\nu}{g \cdot D_{n,50}^2} \tag{A.2}$$

and

$$b = \beta \frac{(1-n)}{n^3} \frac{1}{g \cdot D_{n,50}} \tag{A.3}$$

As was described in section 2.2.2 the discharge through the sample and the water level in the reservoir were measured during the experiment . These two parameters can be used to solve for a and b in equation A.1. For this several properties need to be known, which are defined in table A.1. From left to right: nominal diameter, porosity, kinematic viscosity, sample thickness, sample surface area.

Table A.1: Parameters used for the Forchheimer experiments

Stone class	$D_{n,50}[m]$	$n[-]$	$\nu[m^2/s]$	$dx[m]$	$A_s[m^2]$
Armour	0.044	0.49	$1 \cdot 10^{-6}$	0.28	0.067
Core	0.022	0.43	$1 \cdot 10^{-6}$	0.30	0.067
Toe	0.025	0.42	$1 \cdot 10^{-6}$	0.21 and 0.25	0.067

With these parameters and the measurements the values for a and b and therefore α and β can be computed. This analysis is now performed for one of the experiments with the armour layer stones.

First the water levels and discharges that were measured at the equilibrium points need to be derived. Figure A.1a and A.1b show the time records of these parameters. The equilibrium values are read from the graph and can be found in table A.2

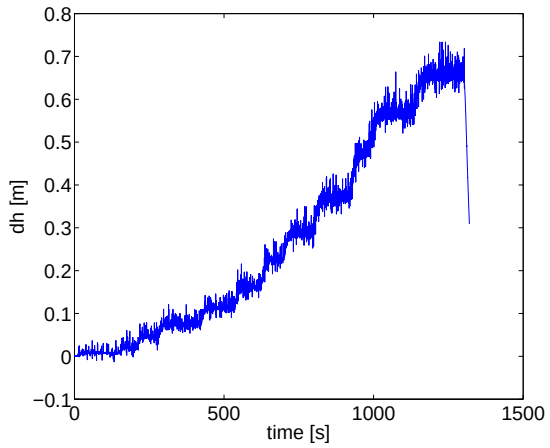

(a) Water level difference during the Forchheimer experiment with armour stones

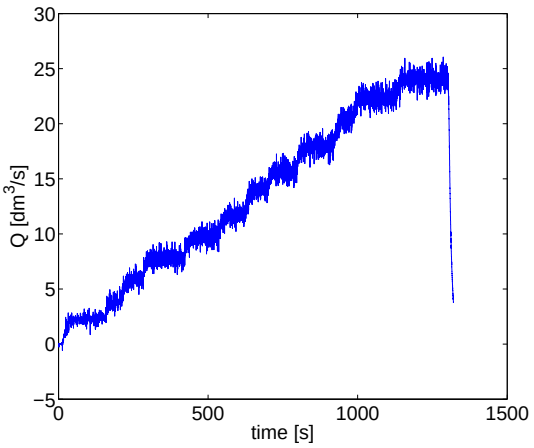

(b) Discharge during the Forchheimer experiment with armour stones

With these values the filter velocity u_f and the gradient i can be determined for each equilibrium point by using $u_f = Q/A_f$ and $i = \frac{dh}{dx}$. Thereafter the two parameters can plotted against each other and a second order polynomial ($y = ax + bx^2$ just like equation A.1) is fitted through the datapoints. Using Excel the values for a and b can then be determined as is shown in figure A.2. For this case $a = 0.2147$ and $b = 17.136$. Now

Table A.2: Equilibrium values for the Forchheimer experiment for the armour stones

Eq. point	1	2	3	4	5	6	7	8	9	10	11	12
$dh[m]$	0.008	0.02	0.045	0.073	0.112	0.16	0.225	0.28	0.362	0.465	0.56	0.648
$Q[dm^3/s]$	2.3	3.8	6.0	7.8	9.8	11.8	14.1	15.7	17.9	20.5	22.4	24.1

equations A.2 and A.3 can be solved for α and β.

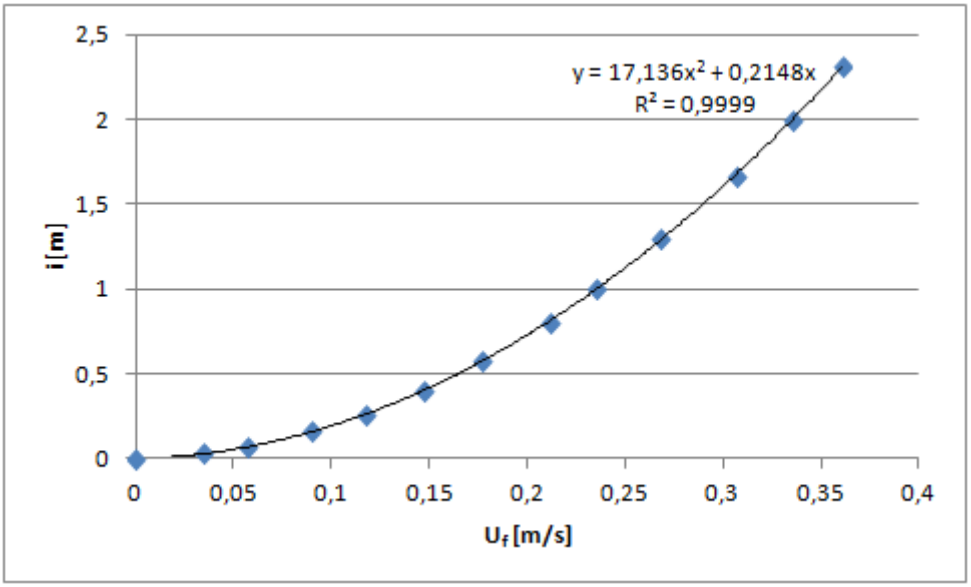

Figure A.2: Fit for the Forchheimer equation for the second test armour stones

A total of eight test were performed and analysed using this procedure: two for the armour stones, four for the core stones and two for the toe stones. There was some spread in the values for α and β, especially for α however since the flow between the stones will be mostly turbulent this should not give too much of a problem. The final values for α and β were obtained by taking the average of the found values per stone class. The results of the Forchheimer experiments are summarised in table A.3

Table A.3: Results of the Forchheimer experiments

	$\alpha[-]$	$\beta[-]$
Armour 1	1816	1.70
Armour 2	1836	1.71
Armour average	**1826**	**1.70**
Core 1	653	1.39
Core 2	830	1.34
Core 3	483	1.35
Core 4	540	1.35
Core average	**627**	**1.36**
Toe 1	496	1.12
Toe 2	688	1.33
Toe average	**591**	**1.23**

Appendix B

Convergence test procedure

This appendix will describe the rationale behind the convergence tests. The test was designed in collaboration with Senne Verpoorten who, as part of his master thesis, was also investigating the IH2VOF model. The aim of the convergence test is to determine the grid size and dimensions for which the model gives an accurate answer with a reasonable computation time. This test was performed for the three mesh parameters: the horizontal grid size Δx, the vertical grid size Δy and the flume length L_f.

For each of the tests a reference case is defined, this is the case with the largest amount of detail (larger computational domain, finer mesh size). The grid dimensions for the reference were taken a lot more detailed than was described in the requirements that were stated in section 3.2. Next the hydraulic conditions of the limiting case (H=0.12 m, T=1.39, h=0.30 m) are defined together with the locations of the wave gauges. It is important for the comparability that the wave gauges for the different cases are positioned at the same positions (w.r.t. the breakwater). After the computations of the reference case and the other cases under consideration have been finished, the results can be compared to find the most appropriate grid dimensions.

The comparison method for the three parameters follow the same principle. The velocity data of a case is compared to that of the reference case for each wave gauge. This is done by comparing the peaks (amplitudes) in the data set with each other. For the convergence tests of the grid cells this procedure can be readily applied, but for the convergence test of the flume length an extra step is required. Since the waves in a longer flume take more time to reach the breakwater, this means that there is an offset in the time it takes before the first wave reaches the structure. A time-shift script is therefore applied which seeks the fifth velocity peak in both datasets and synchronises the two cases. The reason the fifth peak is chosen is that the earlier peaks are rather low which makes the aligning of the two datasets less accurate. This process is visualised in figure B.2 For the determination of the the relative error first the peaks are identified, after which the values of the peaks are subtracted to obtain the difference or error between the two cases. The maximum (absolute) difference is taken as the error for that wave gauge. This procedure is visualised in figure B.1. From this figure it can be seen that there are some small shifts between the two cases. This is the reason why the difference in peak height is calculated, rather than taking the difference between the two velocity signals as this would have given a distorted view. In the figure the location where the largest difference occurs is marked with a circle. With largest peak height difference per wave gauge known, the relative error is then defined as the peak height difference divided by the height of the peak. Finally the relative error of the entire case is determined by taking the average of the relative errors per wave gauge.

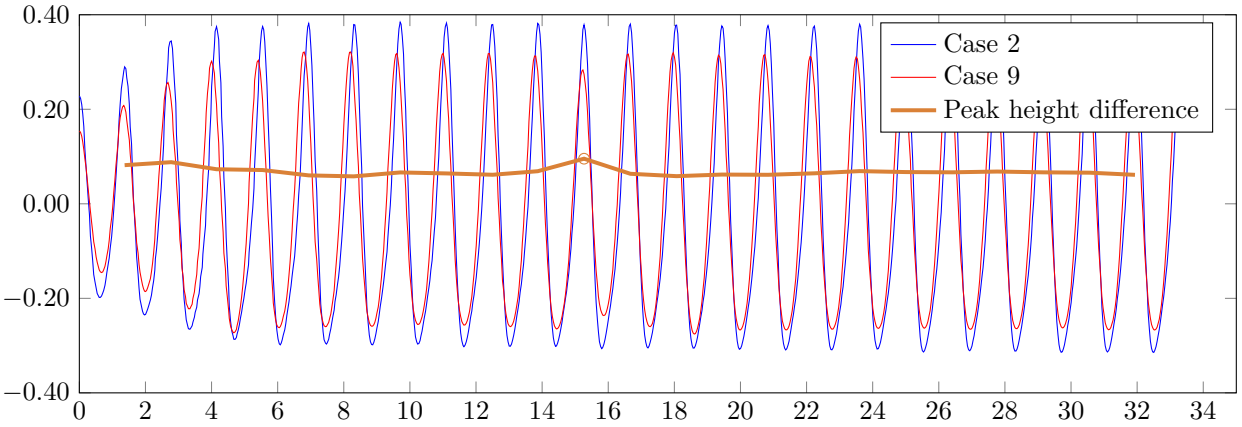

Figure B.1: Peak differences between two cases for a certain wave gauge

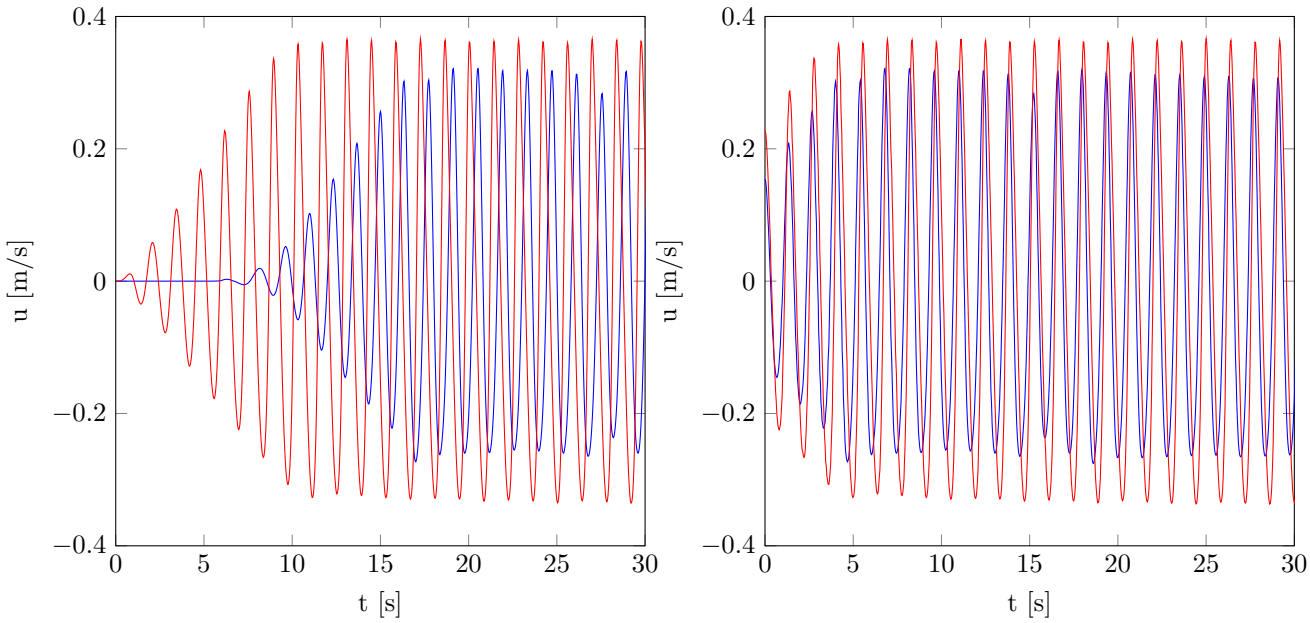

(a) Before time-shift

(b) After time-shift

Figure B.2: Time-shift

Appendix C

Peak and trough analysis

This appendix presents the peak and trough analysis that was performed. Table C.2 shows the results of the peak comparison and table C.3 the results of the trough comparison. The first two columns show test or experiment identification. Columns 3 to 8 show the root-mean-square (rms) value of each of the parameter. Columns 9 to 14 finally show the error between the rms values of IH2VOF and the measurements. As was discussed before, during the flume experiments several tests with the same wave conditions have been performed. Therefore several measurements can be compared to the same IH2VOF computation. In addition to the individual errors of the measurements the average error of the measurements compared to the corresponding computation is determined. It should be noted here that measurements R001 to R014 are not used in the computation of the average error, because during these experiments some difficulties with the equipment occurred leading to potential errors.

The information obtained by the peak analysis can also be used to determine the characteristic wave height of the different measurements and computations. This is done by using the data of the wave gauge nearest to the wave generator and taking the sum of the peak and the trough. Thereafter the error is computed, if there are more measurements per computation the average of these errors is also computed. The results are shown in table C.4.

Before the two analyses were performed, the influence of the porosity was determined. In section 2.2.1 it was noted that the determined porosity of the armour layer may be a little too high. Therefore two IH2VOF runs, based on T006, were performed which were identical apart from the porosity of the armour layer. The porous flow properties α and β have also been adapted accordingly. The results are shown in table C.1, where it can be seen that the difference is less than 1% and therefore negligible.

Table C.1: Influence of a different armour porosity on the results of IH2VOF

	T006	T006a	Error [%]
n	0.49	0.44	
α	1826.00	1097.00	
β	1.70	1.12	
rms u_{toe}	0.63	0.62	-0.50
rms p_{front}	3027.20	3024.30	-0.10
rms p_{middle}	3058.10	3056.10	-0.07
rms p_{above}	2336.60	2334.60	-0.09
rms η_{toe}	0.07	0.07	0.03
rms η_{wg}	0.08	0.08	-0.34

Table C.2: Peak comparison

Test	**Measurement**	u_{toe} **[m/s]**	p_{front} **[Pa]**	p_{middle} **[Pa]**	p_{above} **[Pa]**	η_{toe} **[m]**	η_{wg} **[m]**	**Error** u_{toe} [%]	**Error** p_{front} [%]	**Error** p_{middle} [%]	**Error** p_{above} [%]	**Error** η_{toe} [%]	**Error** η_{wg} [%]
T001		0.466	2429.8	2456.0	1981.4	0.057	0.063						
	R001	0.482	2033.8	1989.4	2391.7	0.056	0.087	3.34	-19.47	-23.45	17.16	-0.47	27.97
T002		0.610	2447.7	2445.2	1974.1	0.054	0.060						
	R003	0.704	2196.9	2171.9	2656.5	0.075	0.092	13.42	-11.42	-12.58	25.69	27.69	34.81
	R010	0.746	2192.2	2236.7	2662.9	0.072	0.087	18.29	-11.65	-9.32	25.87	24.49	31.18
	R011	0.741	2250.0	2241.4	2663.5	0.074	0.093	17.77	-8.79	-9.09	25.88	26.86	35.40
	R012	0.740	2243.0	2246.5	2669.7	0.075	0.094	17.65	-9.13	-8.84	26.06	27.34	35.91
	Average							16.78	-10.25	-9.96	25.87	26.60	34.32
T003		0.602	2516.9	2547.9	2069.6	0.063	0.075						
	R002	0.718	2131.2	2041.0	2537.0	0.059	0.084	16.10	-18.10	-24.84	18.42	-6.85	10.18
	R009	0.807	2100.1	2150.7	2615.2	0.060	0.085	25.33	-19.85	-18.47	20.86	-4.94	11.19
	R043	0.681	2129.7	2146.5	2549.3	0.062	0.086	11.51	-18.18	-18.70	18.82	-2.35	12.72
	Average							11.51	-18.18	-18.70	18.82	-2.35	12.72
T004		0.632	2467.1	2448.3	1983.4	0.051	0.079						
	R004	0.805	2291.0	2327.0	2951.3	0.101	0.087	21.55	-7.69	-5.21	32.80	49.73	9.86
	R013	0.733	2381.0	2403.2	2943.7	0.102	0.086	13.80	-3.62	-1.88	32.62	50.51	8.50
	R015	0.804	2347.5	2390.6	2952.9	0.101	0.089	21.48	-5.09	-2.41	32.83	50.13	11.23
	R044	0.774	2419.8	2407.8	3018.9	0.106	0.085	18.36	-1.95	-1.68	34.30	52.23	7.53
	Average							19.92	-3.52	-2.05	33.57	51.18	9.38
T005		0.628	2500.1	2526.1	2047.5	0.060	0.072						
	R005	0.808	2138.1	2140.0	2693.9	0.069	0.104	22.34	-16.93	-18.04	23.99	12.23	30.74
	R014	0.913	2180.1	2214.9	2792.2	0.074	0.102	31.22	-14.68	-14.05	26.67	17.94	29.56
	R045	0.788	2196.3	2221.9	2739.5	0.074	0.102	20.33	-13.83	-13.69	25.26	18.82	29.12
	R046	0.832	2178.1	2224.5	2732.4	0.075	0.106	24.53	-14.78	-13.56	25.07	19.58	32.11
	Average							22.43	-14.31	-13.62	25.16	19.20	30.62
T006		0.627	3027.2	3058.1	2575	0.066	0.083						
	R006	0.667	2631.4	2613.6	3232.8	0.082	0.096	6.06	-15.04	-17.01	20.35	19.43	13.67
	R016	0.672	2682.1	2693.7	3187.8	0.077	0.096	6.77	-12.87	-13.53	19.22	14.69	14.01
	R040	0.676	2649.9	2679.9	3191.0	0.077	0.095	7.29	-14.24	-14.11	19.30	14.44	13.00
	Average							7.03	-13.55	-13.82	19.26	14.56	13.51
T007		0.606	3140.7	3117.5	2656.1	0.095	0.115						

Continued on next page

Table C.2 – continued from previous page

Test	**Measurement**	u_{toe} **[m/s]**	p_{front} **[Pa]**	p_{middle} **[Pa]**	p_{above} **[Pa]**	η_{toe} **[m]**	η_{wg} **[m]**	**Error** u_{toe} [%]	**Error** p_{front} [%]	**Error** p_{middle} [%]	**Error** p_{above} [%]	**Error** η_{toe} [%]	**Error** η_{wg} [%]
	R007	0.887	2870.4	2913.3	3636.6	0.110	0.149	31.71	-9.42	-7.01	26.96	13.84	22.62
	R017	0.853	2933.7	2949.9	3546.9	0.106	0.140	28.96	-7.06	-5.68	25.11	10.11	17.75
	R041	0.879	2914.2	2918.3	3542.8	0.107	0.144	31.05	-7.77	-6.83	25.03	11.43	19.98
	Average							30.01	-7.41	-6.25	25.07	10.77	18.87
T008		0.666	3118.3	3136.6	2653.6	0.066	0.085						
	R008	0.817	2655.7	2693.5	3339.2	0.085	0.139	18.49	-17.42	-16.45	20.53	22.38	38.60
	R018	0.804	2743.8	2760.4	3314.0	0.085	0.138	17.24	-13.65	-13.63	19.93	22.61	38.16
	R019	0.825	2734.6	2758.6	3354.6	0.086	0.140	19.31	-14.03	-13.70	20.90	23.22	38.96
	R039	0.804	2701.2	2752.9	3322.4	0.086	0.138	17.22	-15.44	-13.94	20.13	22.98	37.98
	R042	0.820	2706.7	2756.2	3378.0	0.088	0.134	18.84	-15.21	-13.80	21.44	24.70	36.49
	Average							18.15	-14.58	-13.77	20.60	23.38	37.90
T009		0.529	3234.3	3206.4	2746	0.060	0.080						
	R020	0.723	3100.7	3108.3	3576.3	0.089	0.125	26.84	-4.31	-3.16	23.22	32.76	36.20
T010		0.735	3454.7	3470.0	2987.3	0.098	0.110						
	R022	0.744	3016.3	3027.8	3560.5	0.087	0.174	1.17	-14.53	-14.60	16.10	-11.68	36.60
T011		0.644	3547.0	3486.1	3061.2	0.110	0.127						
	R021	0.837	3246.8	3296.4	3832.1	0.109	0.196	23.09	-9.25	-5.75	20.12	-0.95	35.19
	R047	0.810	3195.1	3224.9	3737.2	0.107	0.192	20.47	-11.01	-8.10	18.09	-3.35	33.84
	Average							21.78	-10.13	-6.93	19.10	-2.15	34.51
T012		0.652	3370.4	3390.7	2904.7	0.056	0.076						
	R024	0.768	3031.8	3005.9	3585.6	0.086	0.120	15.07	-11.17	-12.80	18.99	34.80	36.54
	R049	0.790	3042.7	3038.8	3608.1	0.087	0.114	17.46	-10.77	-11.58	19.50	35.53	33.08
	Average							16.26	-10.97	-12.19	19.24	35.16	34.81
T013		0.736	3407.9	3413.6	2930.8	0.074	0.091						
	R023	0.875	3094.7	3110.3	3847.0	0.115	0.146	15.92	-10.12	-9.75	23.82	35.38	37.76
	R048	0.881	3125.7	3139.0	3882.2	0.113	0.140	16.45	-9.03	-8.75	24.51	34.02	35.13
	Average							16.18	-9.57	-9.25	24.16	34.70	36.45
T014		0.679	3448.8	3463.4	2980.9	0.073	0.091						
	R025	0.892	3128.7	3109.9	3705.0	0.093	0.126	23.80	-10.23	-11.37	19.54	21.48	27.89
	R050	0.865	3058.6	3084.9	3640.8	0.089	0.124	21.45	-12.76	-12.27	18.13	18.48	26.61
	Average							22.63	-11.49	-11.82	18.83	19.98	27.25
T015		0.541	3597.0	3620.4	3141.5	0.073	0.082						

Continued on next page

Table C.2 – continued from previous page

Test	**Measurement**	u_{toe} **[m/s]**	p_{front} **[Pa]**	p_{middle} **[Pa]**	p_{above} **[Pa]**	η_{toe} **[m]**	η_{wg} **[m]**	**Error** u_{toe} [%]	**Error** p_{front} [%]	**Error** p_{middle} [%]	**Error** p_{above} [%]	**Error** η_{toe} [%]	**Error** η_{wg} [%]
	R026	0.550	3189.7	3145.0	3394.4	0.055	0.106	1.66	-12.77	-15.12	7.45	-33.09	23.16
T016		0.620	3588.7	3613.6	3126.1	0.057	0.072						
	R027	0.697	3223.4	3232.8	3803.2	0.092	0.103	11.09	-11.33	-11.78	17.80	37.36	30.26
	R028	0.679	3227.3	3230.5	3811.2	0.093	0.101	8.74	-11.20	-11.86	17.98	38.32	29.33
	R051	0.820	3295.4	3267.7	3913.3	0.093	0.139	24.48	-8.90	-10.59	20.12	38.36	48.72
	Average							14.77	-10.48	-11.41	18.63	38.01	36.11
T017		0.694	3640.8	3652.3	3170.9	0.094	0.106						
	R031	0.765	3259.0	3268.9	3875.3	0.097	0.159	9.35	-11.72	-11.73	18.18	3.33	33.01
	R054	0.767	3281.0	3296.0	3975.3	0.102	0.159	9.52	-10.97	-10.81	20.23	8.29	33.20
	Average							9.44	-11.34	-11.27	19.21	5.81	33.11
T018		0.665	3669.2	3690.1	3206.6	0.073	0.094						
	R029	0.849	3285.0	3279.4	3928.3	0.093	0.139	21.61	-11.70	-12.52	18.37	21.95	32.63
	R052	0.836	3286.6	3292.8	3896.9	0.090	0.140	20.43	-11.64	-12.07	17.71	19.43	33.09
	Average							21.02	-11.67	-12.29	18.04	20.69	32.86
T019		0.725	3629.6	3634.8	3148.6	0.062	0.082						
	R032	0.861	3375.8	3378.5	4263.1	0.132	0.113	15.81	-7.52	-7.59	26.14	53.16	27.98
	R055	0.774	3270.8	3295.9	3921.7	0.101	0.156	6.33	-10.97	-10.28	19.71	38.68	47.71
	Average							11.07	-9.24	-8.93	22.93	45.92	37.84
T020		0.687	3733.7	3748.9	3265.1	0.076	0.097						
	R030	0.837	3322.3	3336.7	4044.4	0.106	0.157	17.87	-12.38	-12.35	19.27	28.42	38.01
	R053	0.870	3334.1	3336.7	4006.7	0.105	0.154	21.01	-11.99	-12.35	18.51	28.03	36.89
	Average							19.44	-12.18	-12.35	18.89	28.23	37.45
T021		0.633	4228.1	4244.9	3762	0.077	0.104						
	R033	0.731	3785.3	3757.9	4092.9	0.067	0.165	13.44	-11.70	-12.96	8.08	-14.06	37.14
	R056	0.786	3776.8	3754.8	4094.1	0.065	0.169	19.50	-11.95	-13.05	8.11	-17.66	38.58
	Average							16.47	-11.82	-13.01	8.10	-15.86	37.86
T022		0.613	4349.6	4111.5	3819.6	0.152	0.150						
	R035	0.881	4099.2	4120.1	5060.1	0.155	0.124	30.34	-6.11	0.21	24.52	1.65	-21.18
	R058	0.860	4025.8	3944.1	4861.7	0.148	0.122	28.69	-8.04	-4.24	21.43	-2.93	-22.99
	Average							29.52	-7.08	-2.02	22.98	-0.64	-22.08
T023		0.707	4268.0	4291.1	3804.2	0.090	0.116						
	R034	0.827	3826.6	3829.0	4365.4	0.094	0.195	14.56	-11.54	-12.07	12.86	4.26	40.27

Continued on next page

Table C.2 – continued from previous page

Test	**Measurement**	u_{toe} **[m/s]**	p_{front} **[Pa]**	p_{middle} **[Pa]**	p_{above} **[Pa]**	η_{toe} **[m]**	η_{wg} **[m]**	**Error** u_{toe} [%]	**Error** p_{front} [%]	**Error** p_{middle} [%]	**Error** p_{above} [%]	**Error** η_{toe} [%]	**Error** η_{wg} [%]
	R038	0.856	3862.9	3837.1	4415.2	0.094	0.192	17.44	-10.49	-11.83	13.84	3.71	39.56
	R057	0.832	3805.8	3813.1	4421.7	0.102	0.191	15.07	-12.14	-12.54	13.97	11.15	38.97
	Average							15.69	-11.39	-12.15	13.55	6.38	39.60
T024		0.783	4234.5	4232.5	3751.4	0.094	0.117						
	R036	0.886	3920.7	3916.6	4783.2	0.129	0.193	11.72	-8.00	-8.07	21.57	26.66	39.47
	R037	0.925	3886.6	3886.7	4719.5	0.123	0.196	15.44	-8.95	-8.90	20.51	23.24	40.40
	R059	0.894	3887.3	3917.1	4781.1	0.126	0.191	12.45	-8.93	-8.05	21.54	24.99	38.98
	Average							13.20	-8.63	-8.34	21.21	24.96	39.62
T025		0.459	4725.1	4739.1	4260.7	0.079	0.081						
	R060	0.595	4268.1	4251.6	4447.4	0.059	0.130	22.74	-10.71	-11.47	4.20	-32.58	37.79
T026		0.506	4815.5	4707.3	4285.3	0.154	0.159						
	R061	0.827	4097.1	4435.8	5329.7	0.145	0.133	38.80	-17.53	-6.12	19.60	-6.28	-19.20
T027		0.653	4699.8	4719.8	4234.1	0.080	0.111						
	R062	0.753	4356.2	4354.2	4870.7	0.094	0.111	13.30	-7.89	-8.40	13.07	15.58	0.57
T028		0.571	4812.8	4880.4	4396	0.096	0.118						
	R063	0.836	4354.8	4361.7	5131.5	0.123	0.157	31.62	-10.52	-11.89	14.33	21.72	25.01

Table C.3: Trough comparison

Test	**Measurement**	u_{toe} **[m/s]**	p_{front} **[Pa]**	p_{middle} **[Pa]**	p_{above} **[Pa]**	η_{toe} **[m]**	η_{wg} **[m]**	**Error** u_{toe} [%]	**Error** p_{front} [%]	**Error** p_{middle} [%]	**Error** p_{above} [%]	**Error** η_{toe} [%]	**Error** η_{wg} [%]
T001		0.307	1775.5	1776.7	1308.8	0.028	0.051						
	R001	0.373	1517.4	1549.4	1335.4	0.046	0.048	17.72	-17.01	-14.67	1.99	38.34	-6.79
T002		0.369	1558.6	1616.6	1125	0.052	0.067						
	R003	0.401	1355.9	1340.2	1248.4	0.062	0.054	8.03	-14.95	-20.62	9.88	16.24	-23.93
	R010	0.386	1325.1	1252.0	1168.5	0.062	0.053	4.30	-17.62	-29.12	3.72	16.58	-24.49
	R011	0.376	1276.2	1270.6	1183.3	0.062	0.055	1.79	-22.13	-27.23	4.93	17.47	-21.10
	R012	0.375	1270.4	1248.4	1165.9	0.062	0.054	1.65	-22.69	-29.49	3.51	16.69	-22.34
	Average							3.94	-19.35	26.62	5.51	16.74	-22.96
T003		0.351	1784.5	1792.6	1314.4	0.025	0.065						
	R002	0.461	1440.5	1397.4	1175.4	0.067	0.055	23.94	-23.88	-28.28	-11.83	62.23	-17.72
	R009	0.426	1471.7	1335.2	1163.7	0.066	0.054	17.66	-21.25	-34.26	-12.95	61.64	-19.89
	R043	0.469	1422.4	1344.4	1180.3	0.066	0.056	25.23	-25.46	-33.34	-11.36	61.70	-16.06
	Average							25.23	-25.46	-33.34	-11.36	61.70	-16.06
T004		0.563	1371.6	1420.8	929.79	0.071	0.087						
	R004	0.525	1287.7	1274.8	1237.9	0.067	0.048	-7.25	-6.52	-11.45	24.89	-6.27	-79.53
	R013	0.466	1179.5	1143.6	1118.2	0.067	0.049	-20.78	-16.29	-24.24	16.85	-6.16	-78.10
	R015	0.519	1251.9	1209.8	1241.3	0.067	0.047	-8.38	-9.56	-17.44	25.10	-5.88	-82.67
	R044	0.558	1157.2	1137.6	1126.3	0.069	0.049	-0.79	-18.53	-24.89	17.45	-3.57	-78.43
	Average							-4.59	-14.04	-21.17	21.27	-4.72	-80.55
T005		0.398	1756.7	1775.3	1311.2	0.030	0.069						
	R005	0.555	1352.0	1297.5	1154.1	0.071	0.046	28.33	-29.93	-36.82	-13.61	57.27	-49.98
	R014	0.494	1302.8	1171.0	1112.9	0.072	0.045	19.42	-34.84	-51.61	-17.82	57.97	-52.05
	R045	0.552	1285.4	1225.5	1149.4	0.071	0.044	27.97	-36.67	-44.86	-14.08	57.65	-56.72
	R046	0.554	1255.8	1219.1	1145.3	0.071	0.043	28.14	-39.89	-45.62	-14.49	57.64	-59.25
	Average							28.06	-38.28	-45.24	-14.28	57.64	-57.98
T006		0.378	2190.5	2178.0	1712.2	0.037	0.077						
	R006	0.417	1960.0	1881.3	1595.5	0.071	0.058	9.36	-11.76	-15.77	-7.31	47.33	-32.12
	R016	0.423	1908.1	1823.7	1584.2	0.071	0.060	10.58	-14.80	-19.43	-8.08	47.84	-28.41
	R040	0.434	1869.3	1813.7	1588.7	0.071	0.059	12.98	-17.18	-20.09	-7.77	47.68	-30.41
	Average							11.78	-15.99	-19.76	-7.93	47.76	-29.41
T007		0.566	1855.3	1939.9	1447.5	0.061	0.110						

Continued on next page

Table C.3 – continued from previous page

Test	**Measurement**	u_{toe} **[m/s]**	p_{front} **[Pa]**	p_{middle} **[Pa]**	p_{above} **[Pa]**	η_{toe} **[m]**	η_{wg} **[m]**	**Error** u_{toe} [%]	**Error** p_{front} [%]	**Error** p_{middle} [%]	**Error** p_{above} [%]	**Error** η_{toe} [%]	**Error** η_{wg} [%]
	R007	0.432	1644.1	1641.4	1439.5	0.090	0.066	-30.97	-12.85	-18.19	-0.56	31.59	-67.75
	R017	0.453	1628.8	1559.6	1474.1	0.084	0.065	-25.14	-13.91	-24.38	1.80	27.35	-69.46
	R041	0.448	1569.1	1512.0	1394.7	0.088	0.065	-26.53	-18.24	-28.30	-3.79	30.29	-69.49
	Average							-25.84	-16.07	-26.34	-0.99	28.82	-69.47
T008		0.424	2239.7	2222.1	1776.4	0.034	0.085						
	R008	0.549	1833.1	1712.6	1503.6	0.083	0.081	22.66	-22.18	-29.75	-18.14	59.33	-4.97
	R018	0.551	1739.5	1657.5	1498.7	0.084	0.082	22.98	-28.76	-34.06	-18.53	59.87	-3.31
	R019	0.550	1681.1	1656.3	1520.2	0.082	0.081	22.81	-33.23	-34.16	-16.85	59.16	-4.76
	R039	0.529	1721.1	1666.8	1526.1	0.081	0.080	19.86	-30.13	-33.32	-16.40	58.34	-5.39
	R042	0.524	1738.4	1658.9	1505.6	0.082	0.079	19.02	-28.84	-33.95	-17.99	59.10	-6.67
	Average							21.17	-30.24	-33.87	-17.44	59.12	-5.03
T009		0.495	2238.5	2319.6	1839.9	0.059	0.112						
	R020	0.440	1926.4	1862.9	1872.7	0.079	0.076	-12.44	-16.20	-24.52	1.75	24.99	-46.00
T010		0.403	2361.9	2462.2	1971.3	0.048	0.099						
	R022	0.511	2031.6	1940.0	1904.0	0.077	0.070	21.17	-16.26	-26.92	-3.53	37.44	-41.36
T011		0.604	2096.9	2195.8	1704.5	0.064	0.127						
	R021	0.497	1814.3	1714.9	1638.3	0.094	0.072	-21.61	-15.58	-28.04	-4.04	31.30	-76.21
	R047	0.506	1755.8	1721.2	1693.4	0.094	0.075	-19.33	-19.43	-27.57	-0.66	31.48	-68.68
	Average							-20.47	-17.50	-27.81	-2.35	31.39	-72.45
T012		0.443	2412.6	2394.1	1948.5	0.050	0.102						
	R024	0.470	2121.6	2018.0	1803.7	0.079	0.071	5.73	-13.72	-18.64	-8.03	36.27	-43.64
	R049	0.449	2059.6	2028.8	1812.6	0.077	0.071	1.37	-17.14	-18.01	-7.50	35.27	-43.42
	Average							3.55	-15.43	-18.32	-7.76	35.77	-43.53
T013		0.466	2200.6	2281.4	1794.2	0.072	0.106						
	R023	0.526	1810.0	1750.3	1646.0	0.094	0.071	11.29	-21.58	-30.34	-9.00	23.89	-49.30
	R048	0.520	1809.8	1770.8	1655.0	0.095	0.072	10.38	-21.59	-28.83	-8.41	24.32	-46.95
	Average							10.83	-21.59	-29.59	-8.71	24.10	-48.12
T014		0.418	2510.2	2486.5	2049.1	0.038	0.098						
	R025	0.528	1957.2	1826.4	1732.9	0.086	0.069	20.78	-28.25	-36.14	-18.25	55.65	-42.93
	R050	0.547	1967.1	1880.4	1732.7	0.087	0.070	23.57	-27.61	-32.23	-18.26	55.94	-39.84
	Average							22.17	-27.93	-34.19	-18.25	55.80	-41.38
T015		0.308	2706.4	2712.2	2235.6	0.038	0.061						

Continued on next page

Table C.3 – continued from previous page

Test	**Measurement**	u_{toe} **[m/s]**	p_{front} **[Pa]**	p_{middle} **[Pa]**	p_{above} **[Pa]**	η_{toe} **[m]**	η_{wg} **[m]**	**Error** u_{toe} [%]	**Error** p_{front} [%]	**Error** p_{middle} [%]	**Error** p_{above} [%]	**Error** η_{toe} [%]	**Error** η_{wg} [%]
	R026	0.414	2369.5	2420.4	2260.7	0.054	0.075	25.61	-14.22	-12.06	1.11	29.50	18.27
T016		0.419	2620.6	2603.6	2152	0.054	0.095						
	R027	0.425	2313.7	2247.6	2133.5	0.063	0.064	1.35	-13.26	-15.84	-0.87	14.85	-48.88
	R028	0.420	2372.3	2293.2	2129.2	0.064	0.063	0.16	-10.47	-13.54	-1.07	15.18	-49.46
	R051	0.554	2172.8	2102.6	1907.5	0.088	0.076	24.26	-20.61	-23.83	-12.82	39.06	-25.43
	Average							8.59	-14.78	-17.73	-4.92	23.03	-41.26
T017		0.379	2557.7	2653.4	2163.6	0.058	0.095						
	R031	0.440	2143.5	2145.0	2093.0	0.077	0.071	13.86	-19.32	-23.70	-3.37	24.08	-35.26
	R054	0.445	2142.6	2117.1	2007.3	0.077	0.071	14.83	-19.37	-25.33	-7.79	24.45	-34.84
	Average							14.35	-19.35	-24.52	-5.58	24.26	-35.05
T018		0.399	2699.9	2676.9	2235.2	0.041	0.100						
	R029	0.539	2185.7	2089.4	1902.5	0.089	0.075	25.96	-23.53	-28.12	-17.49	53.42	-32.64
	R052	0.551	2144.8	2073.1	1900.9	0.089	0.073	27.58	-25.88	-29.13	-17.59	53.71	-36.06
	Average							26.77	-24.70	-28.62	-17.54	53.57	-34.35
T019		0.521	2418.0	2499.1	2017	0.074	0.120						
	R032	0.513	1999.6	1937.2	1834.3	0.096	0.058	-1.65	-20.92	-29.01	-9.96	22.71	-105.50
	R055	0.434	2137.0	2144.1	1997.8	0.078	0.072	-20.01	-13.15	-16.56	-0.96	4.69	-65.85
	Average							-10.83	-17.04	-22.78	-5.46	13.70	-85.67
T020		0.429	2728.3	2698.6	2265.4	0.042	0.105						
	R030	0.510	2164.0	2101.8	1907.3	0.087	0.089	15.92	-26.08	-28.39	-18.78	52.37	-17.20
	R053	0.509	2160.8	2052.0	1895.3	0.089	0.088	15.74	-26.26	-31.51	-19.53	53.37	-19.66
	Average							15.83	-26.17	-29.95	-19.15	52.87	-18.43
T021		0.416	3104.3	3085.6	2645.2	0.050	0.093						
	R033	0.482	2759.3	2758.9	2481.0	0.078	0.095	13.70	-12.50	-11.84	-6.62	36.53	1.92
	R056	0.486	2765.5	2762.2	2484.0	0.078	0.093	14.35	-12.25	-11.71	-6.49	36.11	0.14
	Average							14.03	-12.38	-11.77	-6.55	36.32	1.03
T022		0.505	3005.4	3053.9	2567.5	0.069	0.129						
	R035	0.469	2609.9	2556.7	2720.6	0.115	0.083	-7.67	-15.15	-19.45	5.63	40.20	-55.63
	R058	0.478	2737.9	2780.6	2721.5	0.114	0.079	-5.64	-9.77	-9.83	5.66	39.88	-62.51
	Average							-6.66	-12.46	-14.64	5.64	40.04	-59.07
T023		0.426	3134.6	3093.6	2665.7	0.044	0.115						
	R034	0.543	2691.1	2548.6	2237.6	0.104	0.090	21.52	-16.48	-21.38	-19.13	57.37	-28.60

Continued on next page

Table C.3 – continued from previous page

Test	**Measurement**	u_{toe} **[m/s]**	p_{front} **[Pa]**	p_{middle} **[Pa]**	p_{above} **[Pa]**	η_{toe} **[m]**	η_{wg} **[m]**	**Error** u_{toe} [%]	**Error** p_{front} [%]	**Error** p_{middle} [%]	**Error** p_{above} [%]	**Error** η_{toe} [%]	**Error** η_{wg} [%]
	R038	0.546	2692.7	2537.6	2255.4	0.103	0.086	22.00	-16.41	-21.91	-18.19	56.93	-34.04
	R057	0.540	2700.8	2522.9	2234.0	0.105	0.090	21.17	-16.06	-22.62	-19.32	57.67	-28.07
	Average							21.56	-16.32	-21.97	-18.88	57.32	-30.24
T024		0.625	2832.9	2957.9	2465.2	0.074	0.161						
	R036	0.549	2322.9	2251.1	2098.8	0.117	0.111	-13.82	-21.96	-31.40	-17.46	36.90	-44.18
	R037	0.552	2379.2	2261.5	2110.8	0.118	0.112	-13.24	-19.07	-30.79	-16.79	37.33	-43.82
	R059	0.554	2326.1	2258.2	2070.3	0.120	0.111	-12.71	-21.79	-30.98	-19.07	38.30	-44.78
	Average							-13.26	-20.94	-31.06	-17.77	37.51	-44.26
T025		0.465	3588.5	3583.8	3126.5	0.050	0.060						
	R060	0.394	3239.2	3293.5	3172.5	0.063	0.111	-18.05	-10.78	-8.81	1.45	20.40	45.87
T026		0.491	3445.0	3460.1	2991.3	0.076	0.097						
	R061	0.476	3142.1	3066.0	3218.1	0.114	0.099	-3.25	-9.64	-12.85	7.05	33.59	1.78
T027		0.408	3510.1	3480.8	3045.1	0.057	0.091						
	R062	0.442	3247.2	3266.4	3075.8	0.075	0.083	7.67	-8.10	-6.56	1.00	23.88	-9.28
T028		0.555	3625.6	3630.7	3171	0.050	0.104						
	R063	0.518	3129.7	2989.7	2794.5	0.096	0.085	-7.15	-15.84	-21.44	-13.47	48.21	-22.11

Table C.4: Wave height analysis

Test	Measure-ment	Peak [m]	Trough [m]	H [m]	Error H [%]	Test	Measure-ment	Peak [m]	Trough [m]	H [m]	Error H [%]
T001		0.06	0.05	0.11		T013		0.09	0.11	0.20	
	R001	0.09	0.05	0.13	15.60		R023	0.15	0.07	0.22	9.23
T002		0.06	0.07	0.13			R048	0.14	0.07	0.21	7.19
	R003	0.09	0.05	0.15	13.21		Average				8.21
	R010	0.09	0.05	0.14	10.06	T014		0.09	0.10	0.19	
	R011	0.09	0.05	0.15	14.44		R025	0.13	0.07	0.20	2.92
	R012	0.09	0.05	0.15	14.54		R050	0.12	0.07	0.19	2.58
	Average				13.06		Average				2.75
T003		0.08	0.06	0.14		T015		0.08	0.06	0.14	
	R002	0.08	0.05	0.14	-0.88		R026	0.11	0.07	0.18	30.11
	R009	0.08	0.05	0.14	-0.91	T016		0.07	0.09	0.17	
	R043	0.09	0.06	0.14	1.42		R027	0.10	0.06	0.17	-0.03
	Average				1.42		R028	0.10	0.06	0.16	-1.00
T004		0.08	0.09	0.17			R051	0.14	0.08	0.22	22.68
	R004	0.09	0.05	0.14	-21.94		Average				7.21
	R013	0.09	0.05	0.13	-22.76	T017		0.11	0.10	0.20	
	R015	0.09	0.05	0.14	-21.47		R031	0.16	0.07	0.23	12.02
	R044	0.09	0.05	0.13	-23.68		R054	0.16	0.07	0.23	12.27
	Average				-22.57		Average				12.15
T005		0.07	0.07	0.14		T018		0.09	0.10	0.19	
	R005	0.10	0.05	0.15	6.08		R029	0.14	0.08	0.21	9.72
	R014	0.10	0.05	0.15	4.58		R052	0.14	0.07	0.21	9.33
	R045	0.10	0.04	0.15	3.28		Average				9.53
	R046	0.11	0.04	0.15	5.74	T019		0.08	0.12	0.20	
	Average				4.51		R032	0.11	0.06	0.17	-17.41
T006		0.08	0.08	0.16			R055	0.16	0.07	0.23	11.74
	R006	0.10	0.06	0.15	-3.57		Average				-2.84
	R016	0.10	0.06	0.16	-2.21	T020		0.10	0.10	0.20	
	R040	0.10	0.06	0.15	-3.56		R030	0.16	0.09	0.25	17.96
	Average				-2.88		R053	0.15	0.09	0.24	16.39
T007		0.12	0.11	0.23			Average				17.17
	R007	0.15	0.07	0.21	-5.06	T021		0.10	0.09	0.20	
	R017	0.14	0.07	0.21	-9.91		R033	0.16	0.09	0.26	24.26
	R041	0.14	0.07	0.21	-7.86		R056	0.17	0.09	0.26	24.89
	Average				-8.88		Average				24.58
T008		0.09	0.08	0.17		T022		0.15	0.13	0.28	
	R008	0.14	0.08	0.22	22.59		R035	0.12	0.08	0.21	-34.98
	R018	0.14	0.08	0.22	22.70		R058	0.12	0.08	0.20	-38.55
	R019	0.14	0.08	0.22	22.94		Average				-36.77
	R039	0.14	0.08	0.22	21.98	T023		0.12	0.12	0.23	
	R042	0.13	0.08	0.21	20.46		R034	0.19	0.09	0.28	18.55
	Average				22.02		R038	0.19	0.09	0.28	16.81
T009		0.08	0.11	0.19			R057	0.19	0.09	0.28	17.45
	R020	0.12	0.08	0.20	4.97		Average				17.60
T010		0.11	0.10	0.21		T024		0.12	0.16	0.28	
	R022	0.17	0.07	0.24	14.17		R036	0.19	0.11	0.30	8.86
T011		0.13	0.13	0.25			R037	0.20	0.11	0.31	9.83
	R021	0.20	0.07	0.27	5.33		R059	0.19	0.11	0.30	8.25
	R047	0.19	0.08	0.27	5.05		Average				8.98
	Average				5.19	T025		0.08	0.06	0.14	
T012		0.08	0.10	0.18			R060	0.13	0.11	0.24	41.51
	R024	0.12	0.07	0.19	6.84	T026		0.16	0.10	0.26	
	R049	0.11	0.07	0.18	3.76		R061	0.13	0.10	0.23	-10.25
	Average				5.30	T027		0.11	0.09	0.20	
							R062	0.11	0.08	0.19	-3.64
						T028		0.12	0.10	0.22	
							R063	0.16	0.08	0.24	8.51

Appendix D

IH2VOF remarks

In this appendix some remarks are made concerning the use of the IH2VOF model based on the experience that was obtained during this thesis. Some of these remarks were already mentioned in the core of this report but are repeated to create a more complete overview. Senne Verpoorten also critically looked into the IH2VOF model, so it is advised to look into his report which will be published in 2015.

- When using CORAL to define the geometry, the y-axis is 0 on the top and with a downwards positive y-direction. This is very counter-intuitive.
- Once a mesh is created in CORAL it is relatively easy to adapt the mesh file outside of the CORAL GUI by simply opening the mesh file in notepad and changing the relevant values.
- When defining the wave gauges, make sure the spacing between them is larger than the width of a grid cell. If this is not the case the wave gauges will give a distorted signal or no signal at all.
- When clicking on the *Generate paddle* button, do not proceed with any other settings until this process is done. Wave gauges defined during the generation of the wave paddle will not be saved.
- IH2VOF seems to force the waves into a harmonic form, whereas this is often not the case in flume experiments, where the waves are asymmetric. No solution for this problem was found in this research.
- The model requires a some spin-up time that is dependent on the flume length, this means that the spin-up time of 45 s that is used in this research may be different for other researches
- The interface between the water and construction is a problematic area. A 'boundary layer' will be formed there with a thickness that corresponds with the chosen cell dimensions. The origin of this problem is that those are not exclusively construction, nor exclusively water. Therefore IH2VOF cannot compute the flow here.

Bibliography

Kees Arets. Modellering van de stroomsnelheden bij teen van een golfbreker. 2013.

Melvin Koote and Wilmar Zeelenberg. The use of Elastocoast in breakwater research. 2012.

Ruben B. M. Peters. Stone stability in breakwater toes based on local hydraulic conditions, 2014.

Gerrit J. Schiereck. *Introduction to Bed, bank and shore protection.* Delft University Press, 2004. ISBN 90-407-1683-8.

J. van den Bos, H.J. Verhagen, M. Zijlema, and B. Mellink. Towards a practical application of numerical models to predict wave-structure interaction: an initial validation. 2014.